Revista Internacional de Métodos Numéricos para Cálculo y Diseño en Ingeniería

Analysis of Burr-XII Lifespan Using Adaptive Progressive Type-II Hybrid Binomial Censoring with Physical Modeling of Polyester and Carbon Fibers

Refah Alotaibi[1,*], **Hoda Rezk**[2] **and Ahmed Elshahhat**[3]

[1]Department of Mathematical Sciences, College of Science, Princess Nourah bint Abdulrahman University, Riyadh, 11671, Saudi Arabia

[2]Department of Statistics, Al-Azhar University, Cairo, 11884, Egypt

[3]Faculty of Technology and Development, Zagazig University, Zagazig, 44519, Egypt

ABSTRACT

This study introduces advanced statistical methods, allowing for more efficient and accurate reliability testing of fibers such as polyester and carbon. Polyester ficbers are suitable for textiles and industrial use due to their wrinkle resistance and affordability, while carbon fibers offer superior strength, thermal stability, and corrosion resistance. To guarantee greater efficiency of inference methodologies and reduce overall testing time, the adaptive Type-II progressive hybrid censoring via binomial removals has gained popularity in reliability analysis and life-testing problems. The proposed scheme allows survival units to be removed at random stages according to a binomial law, thereby reducing experimental time while preserving statistical efficiency. When lifetimes are gathered using the suggested censoring technique, point and interval estimates of the unknown parameters of the Burr-XII model are obtained using both classical and Bayesian approaches. We obtain various Bayesian estimates using the squared loss function. Some numerical methods are employed to obtain the suggested estimators due to their complexity. The various Bayes estimates and related credible intervals are created using Markov chain Monte Carlo techniques. To assess estimator performance, extensive simulation studies are conducted, comparing bias, mean squared error, coverage probabilities, and interval lengths under varying censoring and removal settings. The simulation results confirm that the Bayesian framework, particularly with informative priors, provides more accurate and stable estimates than asymptotic likelihood-based methods. We examine two physics data sets representing polyester and carbon fibers to demonstrate the relevance of the suggested approaches in a real-world setting. These applications highlight the practical value of the proposed approach for material design, maintenance planning, and broader reliability engineering problems.

OPEN ACCESS

Received: 13/06/2025

Accepted: 12/09/2025

Published: 23/01/2026

DOI
10.23967/j.rimni.2025.10.69056

Keywords:
Burr-XII
random removal
adaptive censoring
Bayesian Markovian-based
reliability
simulation
physical data modeling

*Correspondence: Refah Alotaibi (rmalotaibi@pnu.edu.sa).

1 Introduction

In life-testing trials, censoring is frequently employed to strike a balance between the number of test units, the efficiency of statistical methods, and the total test duration. However, experiments may be terminated before responses from all test units are obtained, due to time or financial constraints. Such experiments result in censored data. Reliability studies and life-testing experiments frequently employ Type-I (time) and Type-II (failure) censoring schemes. A hybrid censoring strategy combines Type-I and Type-II censoring techniques. These traditional censoring approaches do not allow for the interim removal of surviving units before the endpoint.

A progressive Type-II censoring method (PCS-TII) has been proposed to address this lack of flexibility by permitting the removal of units from the life test at various times other than the termination point. The main advantage of PCS is that it can reduce test duration while still including items with extremely long lifespans in the data. Balakrishnan and Cramer [1] provide more thorough evaluations of PCS-TII. A progressive hybrid censoring scheme (PH-CS), a combination of Type-II progressive and hybrid censoring techniques, was presented by Kundu and Joarder [2]. Similar to PCS-TII, PH-CS terminates the experiment either at a specified number of failures or at a predefined time. This plan was referred to as the Type-I progressive hybrid censoring scheme (PH-CS-TI) by Childs et al. [3]. The drawback of PH-CS-TI, like Type-I censoring, is that very few failures may occur before the predetermined period (or even none at all); as a result, statistical methods may be ineffective or inapplicable. Ng et al. [4] suggested an adaptive Type-II progressive hybrid censoring scheme (APH-CS-TII) to address this issue and improve the efficiency of statistical analysis. This scheme ensures that the total test time does not exceed the predefined time T, while also allowing the researcher to stop the experiment when the desired number of failures is reached.

The APH-CS-TII has received considerable attention and has grown in popularity in reliability analysis and life testing over the past decade. However, in certain real-world scenarios, such as clinical trials, it is impossible to predict the exact design of the removals, and the number of participants who leave the experiment at each stage is random. Consequently, a discrete distribution, such as the discrete uniform or binomial probability distribution, governs the number of participants who withdraw at each stage. Because it assumes that each removal event occurs with equal probability regardless of the number of units removed, the discrete uniform removal design introduced by Yuen and Tse [5] may not be appropriate. Consequently, Tse et al. [6] argued that a more practical approach to modeling the number of events out of n trials is to employ the binomial distribution with success probability pr.

The statistical inference of model parameters for different lifetime distributions under progressive censoring with binomial removals has been investigated in numerous studies. The Type-II progressive censored sampling with binomial removals (PC-SBR-TII) was first introduced by Tse et al. [6]. Type-II progressive interval censoring with binomial removals was studied by Xiang and Tse [7]. The progressive Type-I interval censoring with binomial removals using the accelerated life test was proposed by Ding et al. [8]. The PH-CS-TII with binomial removals was presented by Afify [9]. Estimation problems for the weighted exponential distribution under Type-II progressive censoring with binomial removals were studied by Dey et al. [10]. More recently, the progressive first-failure censoring scheme with binomial removals was introduced by Ashour et al. [11].

The analysis of APH-CS-TII when the number of items eliminated at each stage is random has not, to the best of our knowledge, been studied in the literature. Therefore, to incorporate scenarios where the removals at each stage of the experiment follow the binomial distribution, new models and statistical procedures must be developed. The primary goal of this work is thus to extend from prefixed removals to binomial random removals in order to obtain the adaptive Type-II progressive hybrid censored sample. We refer to this design as the adaptive Type-II progressive hybrid censoring scheme with binomial removals (APH-CSBR-TII).

Specifically, polyester fibers were selected because of their widespread use in textiles and industrial applications, where durability, wrinkle resistance, and cost-effectiveness are critical factors. Carbon fibers, on the other hand, are increasingly applied in aerospace, automotive, and civil engineering industries due to their exceptional tensile strength, thermal stability, and corrosion resistance. These properties make both fiber types representative of two ends of the application spectrum: one focused on consumer and industrial utility, and the other on high-performance engineering demands. Importantly, both fibers are subject to reliability concerns related to their mechanical performance and degradation under stress, making them highly suitable for demonstrating the effectiveness of an APH-CSBR-TII strategy in lifespan modeling. For additional details, see Walker and Thrower [12] and Deopura et al. [13].

The Burr Type-XII (B12) distribution, originally introduced by Burr [14] as a two-parameter family, is recognized for its remarkable flexibility in modeling diverse data structures. This distribution is capable of representing a wide array of distributional shapes, encompassing various well-known families such as gamma, log-normal, log-logistic, and specific forms of beta distributions, including bell-shaped and J-shaped types (but excluding U-shaped structures). Additionally, the Burr distribution arises naturally in several compound distribution settings. For instance: (i) when the scale parameter of a Weibull distribution follows a gamma distribution, the resulting compound model follows a Burr distribution, and (ii) compounding an exponential distribution with a gamma-distributed rate parameter also leads to a Burr formulation; see Goel et al. [15] and Chakraborty et al. [16].

Due to its adaptability, the B12 distribution has been extensively applied across multiple domains, including finance, hydrology, and reliability analysis, for modeling a broad spectrum of real-world data. Empirical datasets effectively captured by the Burr distribution include household income distributions, agricultural price variations, insurance risk assessments, transportation and travel time data, flood magnitude studies, and reliability failure times; see Polosin et al. [17]. As a result, it has recently become one of the most versatile and useful distributions for data analysis and reliability applications.

However, suppose X is a lifetime of product that follows the B12($\boldsymbol{\Omega}$) such that $\boldsymbol{\Omega} = (\sigma, \gamma)$, then its probability density function (PDF) (say, $f(\cdot)$), cumulative distribution function (CDF) (say, $F(\cdot)$), and hazard rate function (HRF), $h(\cdot)$ (at time $t > 0$), are given by

$$f(x; \boldsymbol{\Omega}) = \sigma\gamma x^{\gamma-1}(1 + x^{-\gamma})^{-(\sigma+1)}, \ x > 0, \tag{1}$$

$$F(x; \boldsymbol{\Omega}) = 1 - (1 + x^{\gamma})^{-\sigma}, \tag{2}$$

and

$$h(t; \boldsymbol{\Omega}) = \frac{\sigma\gamma t^{\gamma-1}}{(1 + t^{\gamma})}, \tag{3}$$

respectively, where the associated reliability function (RF) is given by $R(t) = 1 - F(t)$.

When lifetime data are collected under the APH-CSBR-TII scheme, the primary objective of this study is to employ maximum likelihood and Bayesian inferential methodologies to estimate the unknown parameters of the B12 distribution (both point and interval estimation). Based on various balanced-type symmetric and asymmetric loss functions, Bayes estimators are derived under the assumption of independent gamma priors. Since the proposed estimators have complex forms, the Newton–Raphson (NR) algorithm and Markov chain Monte Carlo (MCMC) methods are suggested to obtain the Bayes and classical estimates, along with the corresponding asymptotic and credible intervals. Specifically, the NR method is employed to compute the maximum likelihood estimates (MLEs) using the package, whereas the software, which analyzes MCMC outputs, is used to generate Bayesian estimates. A Monte Carlo simulation is conducted to evaluate the performance of the proposed estimators. For interval estimation, the average interval length and coverage probability are considered to assess efficiency, while for point estimation, the simulated mean squared error and relative absolute bias are employed. Based on the simulation outcomes, several recommendations are provided. Finally, for illustrative purposes, two real datasets are analyzed.

The remainder of the paper is organized as follows. An APH-CSBR-TII formulation is introduced in the next section. Sections 3 and 4 address the classical and Bayesian inference of the unknown parameters, respectively. Section 5 presents the results of the simulation study. Section 6 provides real-data applications, and Section 7 concludes the paper with some final remarks.

2 Design of APH-CSBR-TII

Assume that at time zero, n identical items are placed on a life test, where the progressive censoring scheme $\boldsymbol{r} = (r_1, r_2, \ldots, r_R)$ is predetermined, and the effective number of failures is v $(v < n)$. Suppose the researcher sets an ideal total test time $T \in (0, \infty)$, although the experimental period may extend beyond T. At the time of the first failure, $X_{1:v:n}$, the researcher randomly removes r_1 of the $n-1$ surviving items from the remaining units. Similarly, at the second failure time, $X_{2:v:n}$, r_2 of the $n - r_1 - 2$ remaining items are randomly removed. Although the progressive censoring scheme $\boldsymbol{r}$ is predetermined, some values of r_i, for $i = 1, 2, \ldots, v$, may change during the test. This experiment follows the standard increasingly Type-II right-censored order statistics framework. In Case I, the test stops at the time of the v-th failure if $X_{v:v:n}$ occurs before time T, i.e., if $X_{v:v:n} < T$. Otherwise, the number of progressive removals is adjusted by setting $r_i = 0$ for $i = j + 1, \ldots, v - 1$, where j denotes the number of observed failures occurring before T, such that $X_{j:v:n} < T < X_{j+1:v:n}$. Consequently, the modified number of removals is given by $r_v^* = n - v - j - \sum_{i=1}^{j} r_i$. This process then continues without any further removals, following the standard Type-II censoring approach, and all surviving items are removed at the time of the v-th failure. Notably, the test time T plays a crucial role in determining the number of removals and serves as a trade–off between a shorter experimental duration and a higher likelihood of observing more failures. For further details, see Elshahhat and Mazen [18].

Assume that $X = (X_{1:v:n}, X_{2:v:n}, \ldots, X_{j:v:n}, X_{j+1:v:n}, \ldots, X_{v:v:n})$ denotes the independent lifetimes of the adaptable Type-II progressively hybrid censored order statistics with a predetermined number of removals. Then, letting $\boldsymbol{\Omega}$ be the parameter vector, the joint likelihood function of the observed data, denoted $L_1(\cdot)$, can be expressed as:

$$L_1(\boldsymbol{\Omega}|X) = \rho_j \prod_{i=1}^{v} f(x_{i:v:n}; \boldsymbol{\Omega}) \prod_{i=1}^{j} [R(x_{i:v:n}; \boldsymbol{\Omega})]^{r_i} \left[\bar{F}(x_{v:v:n}; \boldsymbol{\Omega})\right]^{r_R^*}, \tag{4}$$

where $\rho_j = \prod_{i=1}^{v} \left[n - i + 1 - \sum_{d=1}^{\max(i-1,j)} r_d\right]$.

Now, assume that, with a given probability p, each item eliminated from the adaptive Type-II progressive hybrid censored life test is independent of the others. Then, for $i = 1, 2, \ldots, v - 1$, the likelihood of r_i item(s) being withdrawn at the ith failure follows the binomial probability rule with parameters $(n - v - \sum_{k=1}^{i-1} r_k, p)$, as follows:

$$Pr(r_i|r_{i-1},\ldots,r_1) = \binom{n-v-\sum_{k=1}^{i-1} r_k}{r_i} p^{r_i}(1-p)^{n-v-\sum_{k=1}^{i-1} r_k}, \tag{5}$$

where $0 \le r_i \le n-v-\sum_{k=1}^{i-1} r_k$ for $i = 1, 2, \ldots, v-1$; see Elshahhat and Mazen [18].

Thus, the joint probability, say $L_2(\cdot)$, of binomial removals $r_i, i = 1, 2, \ldots, v-1$, is given by:

$$L_2(r;p) = Pr(r_1)Pr(r_2|r_1) \times \cdots \times Pr(r_{v-1}|r_{v-2},\ldots,r_1). \tag{6}$$

When (6) is substituted into (5), we obtain:

$$L_2(r;p) = \frac{(n-v)!}{(n-v-\sum_{i=1}^{v-1} r_i)! \prod_{i=1}^{v-1} r_i!} p^{\sum_{i=1}^{v-1} r_i}(1-p)^{(v-1)(n-v)-\sum_{i=1}^{v-1}(v-1)r_i}. \tag{7}$$

Furthermore, since r is assumed to be independent of X, the complete likelihood function of the APH-CSBR-TII can be expressed as follows:

$$L(\mathbf{\Omega}, p|x, r) = L_1(\mathbf{\Omega}|X)L_2(r;p), \tag{8}$$

where $L_1(\mathbf{\Omega}|X)$ and $L_2(r;p)$ are predefined in (4) and (7), respectively.

It is evident from (4) that $L_1(\cdot)$ does not involve the binomial parameter and may therefore be maximized directly to obtain the MLE $\hat{\mathbf{\Omega}}$ of $\mathbf{\Omega}$. Furthermore, from (7), it is clear that $L_2(\cdot)$ includes p, and by maximizing $L_2(\cdot)$, the MLE $\hat{p}$ of p can be determined. It should be noted that the PC-SBR-TII proposed by Tse et al. [6] arises as a special case of (8) when $T \to \infty$. Table 1 presents the sampling procedure for a life test based on the APH-CSBR-TII. Prior to the start of the experiment, the researcher specifies the effective sample size v and the total number of test units n. However, it is not possible to determine in advance how many surviving units will be removed during the test. Consequently, the number of surviving units removed is modeled using a binomial distribution with parameter p. The complete sampling process for generating the APH-CSBR-TII sample from a life test is summarized in Table 1.

Table 1: Procedure for sampling a life test using APH-CSBR-TII

Case	Stage	Failure item	Removed item(s)	Survival item(s)
I	1	$X_{1:v:n}$	$r_1 \sim Bin(n-v,p)$	$n-r_1-1$
	2	$X_{2:v:n}$	$r_2 \sim Bin(n-v-r_1,p)$	$n-r_1-r_2-2$
	$\vdots$	$\vdots$	$\vdots$	$\vdots$
	$v-1$	$X_{v-1:v:n}$	$r_{v-1} \sim Bin\left(n-v-\sum_{i=1}^{v-2} r_i, p\right)$	$n-v+1-\sum_{i=1}^{v-1} r_i$
	v	$X_{v:v:n}$	$r_R^* \sim Bin\left(n-v-\sum_{i=1}^{v-1} r_i\right)$	0
II	1	$X_{1:v:n}$	$r_1 \sim Bin(n-v,p)$	$n-r_1-1$
	2	$X_{2:v:n}$	$r_2 \sim Bin(n-v-r_1,p)$	$n-r_1-r_2-2$
	$\vdots$	$\vdots$	$\vdots$	$\vdots$
	j	$X_{j:v:n}$	$r_j \sim Bin\left(n-v-\sum_{i=1}^{j-1} r_i\right)$	$n-j-\sum_{i=1}^{j} r_i$
	$j+1$	$X_{j+1:v:n}$	0	$n-j-1-\sum_{i=1}^{j} r_i$

(Continued)

Table 1 (continued)

Case	Stage	Failure item	Removed item(s)	Survival item(s)
	$\vdots$	$\vdots$	$\vdots$	$\vdots$
	$v-1$	$X_{v-1:v:n}$	0	$n-v+1-\sum_{i=1}^{j} r_i$
	v	$X_{v:v:n}$	$r_v^* = n - v - \sum_{i=1}^{j} r_i$	0

3 Likelihood Inference

This section derives the MLEs of $\sigma,\ \gamma,\ p,\ R(t)$, and $h(t)$ under the proposed censoring strategy. Assume that $x_{1:v:n} < \ldots < x_{j:v:n} < T < x_{j+1:v:n} < \ldots < x_{v:v:n}$ are APH-CS-TII order statistics from the B12 population with PDF and CDF given by (1) and (2), respectively, and with binomial removals $r_1, \ldots, r_j, 0, \ldots, 0, n - v - \sum_{i=1}^{j} r_i$. For convenience, throughout this section and those that follow, we write x_i in place of $x_{(i:v:n)}$ for $i = 1, 2, \ldots, v$. By substituting (1) and (2) into (4), the likelihood function can therefore be expressed, up to a proportionality constant, as:

$$L_1(\sigma, \gamma | x, r) \propto (\sigma\gamma)^v \prod_{i=1}^{v} x_i^{(\gamma-1)} (1 + x_i^{\gamma})^{-(\sigma+1)} \prod_{i=1}^{j} (1 + x_i^{\gamma})^{-r_i\sigma} (1 + x_v^{\gamma})^{-r_v^*\sigma}. \tag{9}$$

The associated log-likelihood function $l_1(\cdot) = \log L_1(\cdot)$ of (9) becomes:

$$l_1 \propto v \log\sigma + v \log\gamma + (\gamma - 1) \sum_{i=1}^{v} \log x_i - (\sigma + 1) \sum_{i=1}^{v} \log(1 + x_i^{\gamma}) - r_i \sum_{i=1}^{j} \log(1 + x_i^{\gamma}) - r_v^* \log(1 + x_v^{\gamma}). \tag{10}$$

To obtain the MLEs $\hat{\sigma}$ and $\hat{\gamma}$ of the B12 parameters σ and γ, respectively, the likelihood equations for σ and γ are derived by taking the first partial derivatives of the log-likelihood function l with respect to σ and γ, and then equating them to zero, as follows:

$$\frac{\partial l_1}{\partial\sigma} = \frac{v}{\sigma} - \sum_{i=1}^{v} \log(1 + x_i^{\gamma}) - \sum_{i=1}^{j} r_i \log(1 + x_i^{\gamma}) - r_v^* \log(1 + x_v^{\gamma}), \tag{11}$$

and

$$\frac{\partial l_1}{\partial\gamma} = \frac{v}{\gamma} + \sum_{i=1}^{v} \log x_i - (\sigma + 1) \sum_{i=1}^{v} \frac{x_i^{\gamma} \log x_i}{1 + x_i^{\gamma}} - \sum_{i=1}^{j} r_i\sigma \frac{x_i^{\gamma} \log x_i}{1 + x_i^{\gamma}} - r_v^*\sigma \frac{x_v^{\gamma} \log x_v}{1 + x_v^{\gamma}}, \tag{12}$$

respectively.

By simultaneously solving the two likelihood equations obtained by differentiating (10) with respect to σ and γ, and then equating each result to zero, the MLEs $\hat{\sigma}$ and $\hat{\gamma}$ can be obtained. Since it is not possible to solve analytically for $\hat{\sigma}$ and $\hat{\gamma}$, we employ the Newton–Raphson (NR) method, implemented via the package suggested by Henningsen and Toomet [19], to compute the numerical estimates of $\hat{\sigma}$ and $\hat{\gamma}$.

Starting from the log-likelihood function $l_2(\cdot) = \log L_2(\cdot)$ given in (7), we next differentiate with respect to p. Consequently, the MLE $\hat{p}$ of p can be obtained by maximizing (7) directly. Thus, the log-likelihood function $l_2(\cdot)$ can be expressed as:

$$l_2(r,p) \propto \sum_{i=1}^{v-1} r_i \log p + \left[(v-1)(n-v) - \sum_{i=1}^{v-1} r_i(v-i)\right] \log(1-p). \tag{13}$$

When (13) is differentiated with respect to p and the result is equated to zero, the MLE $\hat{p}$ of p becomes:

$$\hat{p} = \frac{\sum_{i=1}^{v-1} r_i}{(v-1)(n-v) - \sum_{i=1}^{v-1}(v-i-1)r_i}. \tag{14}$$

The respective MLEs of the RF $R(t)$ and the HRF $h(t)$ can be computed directly as follows:

$\hat{R}(t) = (1+t^{\hat{\gamma}})^{-\hat{\sigma}}$, and $\hat{h}(t) = \hat{\sigma}\hat{\gamma} t^{\hat{\gamma}-1}(1+t^{\hat{\gamma}})$.

Under certain regularity conditions, the MLEs $(\hat{\sigma}, \hat{\gamma}, \hat{p})$ are asymptotically distributed as a multivariate normal with mean vector $\Omega = (\sigma, \gamma, p)$ and variance–covariance matrix $\mathbb{I}^{-1}(\hat{\sigma}, \hat{\gamma}, \hat{p})$, where $\mathbb{I}(\hat{\sigma}, \hat{\gamma}, \hat{p})$ denotes the observed Fisher information matrix, given by:

$$\mathbb{I}^{-1}(\hat{\sigma}, \hat{\gamma}, \hat{p}) = \begin{bmatrix} -l_{11} & -l_{12} & 0 \\ -l_{21} & -l_{22} & 0 \\ 0 & 0 & -l_{33} \end{bmatrix}^{-1}_{(\hat{\sigma}, \hat{\gamma}, \hat{p})} = \begin{bmatrix} \hat{\nu}_{11} & \hat{\nu}_{12} & 0 \\ \hat{\nu}_{21} & \hat{\nu}_{22} & 0 \\ 0 & 0 & \hat{\nu}_{33} \end{bmatrix}, \tag{15}$$

where

$$l_{11} = -\frac{v}{\sigma^2},$$

$$l_{22} = -\frac{v}{\gamma^2} - (\sigma+1)\sum_{i=1}^{v} \frac{x_i^{\gamma}(\log(x_i))^2}{(1+x_i^{\gamma})^2} - \sigma \sum_{i=1}^{j} \frac{r_i x_i^{\gamma}(\log(x_i))^2}{(1+x_i^{\gamma})^2} - \frac{r_R^* \sigma x_R^{\gamma}(\log(x_R))^2}{(1+x_R^{\gamma})^2},$$

$$l_{12} = l_{21} = -\sum_{i=1}^{v} \frac{x_i^{\gamma}\log x_i}{1+x_i^{\gamma}} - \sum_{i=1}^{j} r_i \frac{x_i^{\gamma}\log x_i}{1+x_i^{\gamma}} - r_v^* \frac{x_v^{\gamma}\log x_v}{1+x_v^{\gamma}},$$

and

$$l_{33} = -\sum_{i=1}^{v-1} \frac{r_i}{p^2} - \frac{(v-1)(n-v) - \sum_{i=1}^{v-1} r_i(v-i)}{p^2}.$$

It is worth noting that the items $l_{13} = l_{23} = l_{31}$ and the zero value $l_{32} = 0$ arise from the structure of the likelihood function in (8). Since the joint likelihood decomposes as $L(\Omega, p \mid x, r) = L_1(\Omega \mid x, r)\, L_2(r; p)$, the parameter vector $\Omega = (\sigma, \gamma)$ is associated only with L_1, while the binomial parameter p is associated only with L_2. Consequently, the mixed second derivatives of the log-likelihood with respect to (σ, γ) and p vanish, yielding a block-diagonal Fisher information matrix (see, for example, Balakrishnan and Cramer [1], Elshahhat and Nassar [18]).

We also need to obtain the asymptotic variances of $\hat{R}(t)$ and $\hat{h}(t)$, denoted by $\hat{\nu}_{44}$ and $\hat{\nu}_{55}$, respectively, in order to construct their ACIs. To achieve this, we approximate these variances using the delta method; see Greene [20] for further details. Prior to applying this approach, and taking $\varrho(t;\gamma) = (1+t^{-\gamma}),\ t > 0$, we require the following results:

$$\mathbb{S}_1 = -(\varrho(t;\gamma))^{-\sigma} \log(\varrho(t;\gamma)),$$

$$\mathbb{S}_2 = -\sigma(\varrho(t;\gamma))^{-(\sigma+1)} t^{\gamma} \log(t),$$

$$\mathbb{S}_3 = \frac{\sigma\gamma t^{\gamma-2}[(\gamma-1)\varrho(t;\gamma) - \gamma t^{\gamma}]}{(\varrho(t;\gamma))^2},$$

and

$$\mathbb{S}_4 = \frac{\sigma t^{\gamma-1}}{\varrho(t;\gamma)}\left[1 + \gamma\log(t) - \frac{\gamma t^{\gamma}\log(t)}{\varrho(t;\gamma)}\right].$$

Then, the required variances $\hat{\nu}_{44}$ and $\hat{\nu}_{55}$ of $\hat{R}(t)$ and $\hat{h}(t)$ can be approximated as

$$\hat{\nu}_{44} = (\mathbb{S}_1\hat{\nu}_{11} + \mathbb{S}_2\hat{\nu}_{21})\mathbb{S}_1 + (\mathbb{S}_1\hat{\nu}_{12} + \mathbb{S}_2\hat{\nu}_{22})\mathbb{S}_2,$$

and $\hat{\nu}_{55} = (\mathbb{S}_3\hat{\nu}_{11} + \mathbb{S}_4\hat{\nu}_{21})\mathbb{S}_3 + (\mathbb{S}_3\hat{\nu}_{12} + \mathbb{S}_4\hat{\nu}_{22})\mathbb{S}_4$.

From (15), for the parameter vector $\Omega = (\sigma, \gamma, p)^{\top}$, the diagonal elements of $\mathbb{I}^{-1}(\hat{\sigma}, \hat{\gamma}, \hat{p})$ provide the asymptotic variances of the MLEs. Let $100(1-\phi)\%$ denote the nominal confidence level. Then, the $100(1-\phi)\%$ ACIs of Δ_i (for $i = 1, 2, 3, 4, 5$) can be expressed as follows:

$$\left(\hat{\Delta}_i \pm z_{\frac{\phi}{2}}\sqrt{\hat{\nu}_{ii}}\right),\ i = 1, 2, 3, 4, 5,$$

where $(\hat{\Delta}_1, \hat{\Delta}_2, \hat{\Delta}_3, \hat{\Delta}_4, \hat{\Delta}_5) = (\sigma, \gamma, p, R(t), h(t)$ and $z_{\frac{\phi}{2}}$ is the upper $\left(\frac{\phi}{2}\right)$th percentile point of the standard normal distribution.

4 Bayes' Inference

This part develops the Bayes point and credible interval estimates of σ, γ, p, $R(t)$, and $h(t)$ based on the APH-CSBR-TII plan. The analysis is carried out under various settings of p (probability of random removals), T (threshold point), n (total experimental units), and v (failure count).

4.1 Prior PDFs

Before deriving the Bayesian estimators, it is essential to specify suitable prior distributions for the unknown parameters, as these priors reflect initial knowledge and directly shape the resulting posterior inferences. Presume that the two unknown B12($\mathbf{\Omega}$) parameters are independent and have gamma prior distributions; the joint independent gamma density priors of $\mathbf{\Omega}$ become

$$\eta_1(\sigma, \gamma) \propto \sigma^{\xi_1-1}\gamma^{\xi_2-1}e^{-(\zeta_1\sigma+\zeta_2\gamma)},\ \sigma, \gamma > 0, \tag{16}$$

where $\xi_i, \zeta_i > 0$ for $i = 1, 2$.

To analyze the Bayes framework of the binomial parameter p, the Beta (ξ_3, ζ_3) density, which is a powerful model for modeling doubly-bounded data, is utilized, as follows:

$$\eta_2(p) = \frac{1}{B(\xi_3, \zeta_3)}p^{\xi_3-1}(1-p)^{\zeta_3-1},\ 0 < p < 1,\ \xi_3, \zeta_3 > 0, \tag{17}$$

where $B(.,.)$ is beta function.

4.2 Posterior PDFs

By combining prior information with the observed data under the proposed censoring scheme, the joint posterior formulations yield the updated distributions of the unknown parameters for Bayesian inference. By combining (9) with (16) in continuous Bayes' theorem, the joint posterior PDF (say, $\Lambda_1(\cdot)$) of $\mathbf{\Omega}$ becomes

$$\Lambda_1(\sigma,\gamma|x,r) = \mathbb{V}^{-1}\sigma^{\nu+\xi_1-1}\gamma^{\nu+\xi_2-1}e^{-(\zeta_1\sigma+\zeta_2\gamma)} \times \prod_{i=1}^{\nu} x_i^{(\gamma-1)}(1+x_i^{\gamma})^{-(\sigma+1)}\prod_{i=1}^{j}(1+x_i^{\gamma})^{-r_i\sigma}(1+x_\nu^{\gamma})^{-r_\nu^*\sigma}, \tag{18}$$

where $\mathbb{V} = \int_0^\infty\int_0^\infty \eta_1(\sigma,\gamma)\times L_1(\sigma,\gamma|x,r)\mathrm{d}\sigma\mathrm{d}\gamma$.

Due to the intricate nature of Eq. (9), the computation of the double integral ratio in (18) does not yield a straightforward closed-form mathematical solution. Consequently, deriving the Bayes' estimates $(\tilde{\sigma},\tilde{\gamma})$ of (σ,γ) through analytical methods necessitates a numerical approach. To address this challenge, we advocate for the MCMC technique, leveraging the coda package introduced by Plummer et al. [21]. This methodology enables us to generate representative samples from the posterior distribution defined in (18) and subsequently estimate the Bayesian point estimates of σ, γ, $R(t)$, and $h(t)$, along with their associated credible intervals. To effectively implement the MCMC framework, we first express the posterior PDFs of σ and γ from (18) in a separate form, as follows:

$$\Lambda_1^{\sigma}(\sigma|\gamma,x,r) \propto \sigma^{\nu+\xi_1-1}e^{-\zeta_1\sigma}\prod_{i=1}^{\nu}(1+x_i^{\gamma})^{-(\sigma+1)}\prod_{i=1}^{j}(1+x_i^{\gamma})^{-r_i\sigma}(1+x_\nu^{\gamma})^{-r_\nu^*\sigma}, \tag{19}$$

and

$$\Lambda_1^{\gamma}(\gamma|\sigma,x,r) \propto \gamma^{\nu+\xi_2-1}e^{-\zeta_2\gamma}\prod_{i=1}^{\nu}x_i^{(\gamma-1)}(1+x_i^{\gamma})^{-(\sigma+1)}\prod_{i=1}^{j}(1+x_i^{\gamma})^{-r_i\sigma}(1+x_\nu^{\gamma})^{-r_\nu^*\sigma}, \tag{20}$$

respectively.

From (19) and (20), it is evident that simulating random samples from the posterior PDFs of σ and γ is not feasible, as they do not simplify to any known distribution. To address this issue, the subplots in Fig. 1 demonstrate that the posterior PDFs of σ and γ, given in (19) and (20), respectively, can be approximated by a normal distribution. Accordingly, the Metropolis-Hastings (M-H) algorithm with normal proposal distributions is utilized to update samples of σ and γ.

To acquire the MCMC samples of σ and γ and perform the desired inference, follow these steps:

Step 1: Set $j=1$.
Step 2: Set $\left(\sigma^{(0)},\gamma^{(0)}\right) = (\hat{\sigma},\hat{\gamma})$.
Step 3: Generate $\sigma^{(j)}$ from $\Lambda_1^{\sigma}(\sigma^{(j)}|\gamma^{(j-1)},x,r)$, using M-H algorithm as:
  a. Generate σ° from the normal distribution $\eta(\sigma)$.
  b. Obtain $\xi_\sigma = \min\left\{1, \dfrac{\pi_1^{\sigma}\left(\sigma^{\circ}|\,\lambda^{(j)},x,r\right)}{\pi_1^{\sigma}\left(\sigma^{(j-1)}|\,\lambda^{(j)},x,r\right)}\right\}$.
  c. Generate u_σ from uniform $U(0,1)$ distribution.
  d. Set σ° if $u_\sigma \le \xi_\sigma$ otherwise set $\sigma^{(j-1)}$.
Step 4: Redo Step 3 for γ.
Step 5: Putting $\sigma^{(j)}$ and $\gamma^{(j)}$ into $R(t)$ and $h(t)$ to get $R^{(j)}(t)$ and $h^{(j)}(t)$.
Step 6: Put $j=j+1$.
Step 7: Repeat steps 3-6 $\mathcal{T}$ times to get

$$\left[\vartheta^{(1)},\ldots,\vartheta^{(\mathcal{T})}\right],$$

where $\vartheta = \sigma,\gamma,R(t)$ or $h(t)$.

Step 8: Obtain the Bayes estimate of ϑ, where $\bar{\mathcal{T}} = \mathcal{T} - \mathcal{T}^{\circ}$, as follows:

$$\tilde{\vartheta} = \frac{1}{\bar{\mathcal{T}}} \sum_{j=\mathcal{T}^{\circ}+1}^{\mathcal{T}} \vartheta^{(j)},$$

where $\mathcal{T}^{\circ}$ is the burn-in length.

Step 9: To obtain the BCI of ϑ, sort $\left[\vartheta^{(\mathcal{T}^{\circ}+1)}, \ldots, \vartheta^{(\mathcal{T})}\right]$ to be $\left[\vartheta^{[\mathcal{T}^{\circ}+1]}, \ldots, \vartheta^{[\mathcal{T}]}\right]$. Then, the $100(1-\phi)\%$ BCI of ϑ is given by

$$\left\{\vartheta^{\left[\frac{\phi}{2}\bar{\mathcal{T}}\right]}, \vartheta^{\left[\left(1-\frac{\phi}{2}\right)\bar{\mathcal{T}}\right]}\right\}.$$

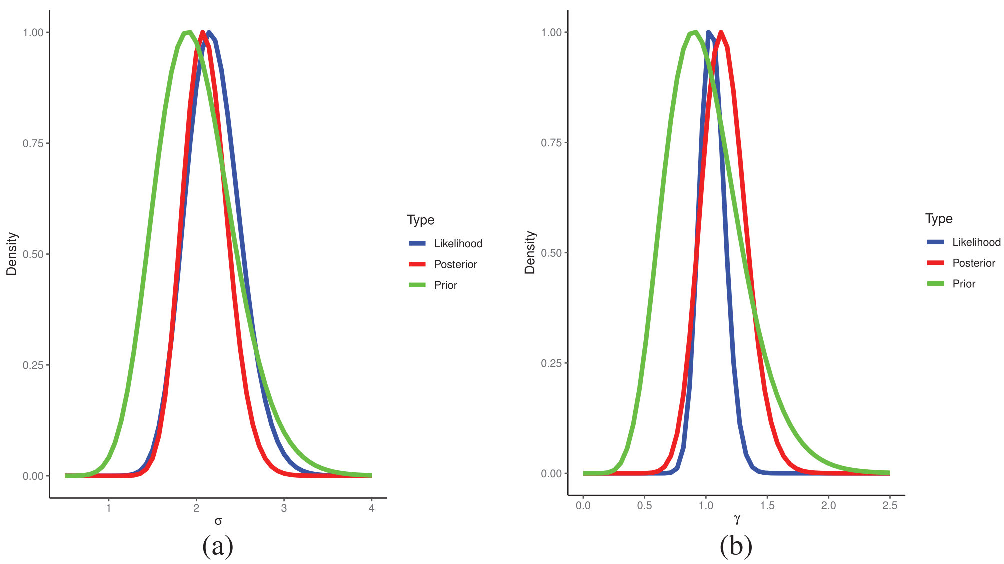

Figure 1: Conditional PDFs of σ (a) and γ (b) when $(p, T) = (0.5, 5)$

Similarly, by combining (7) with (17) in the continuous Bayes' theorem, the joint posterior PDF (denoted by $\Lambda_2(\cdot)$) of p is given by

$$\Lambda_2(p|r) \propto p^{\xi_3^*-1}(1-p)^{\zeta_3^*-1}, \tag{21}$$

where $\xi_3^* = \xi_3 + \sum_{i=1}^{v-1} r_i$ and $\zeta_3^* = \zeta_3 + (v-1)(n-v) - \sum_{i=1}^{v-1} (v-i)r_i$.

Clearly, from (21), samples of p can be generated using any beta-sampling routine. Subsequently, the MCMC-based point and credible interval estimates can be readily obtained.

5 Simulation Comparisons

To assess the performance of the proposed theoretical results for σ, γ, $R(t)$, $h(t)$, and p—derived using likelihood and Bayesian inference methods—comprehensive Monte Carlo simulations are conducted. For this purpose, a total of 1000 APH-CSBR-TII samples are randomly generated from the B12 distribution under two different parameter configurations for the true values of B12(σ, γ), namely Set-1: $(0.2, 0.8)$ and Set-2: $(2, 1)$.

Accordingly, at time $t = 0.1$, the true values of $(R(t), h(t))$ for Set-1 and Set-2 are computed as $(0.9710, 0.2189)$ and $(0.8264, 1.8182)$, respectively. All obtained estimates are further evaluated under various settings of p (probability of random removals), T (threshold point), n (total experimental units), and v (failure count), specifically $p = 0.4, 0.8$, $n = 40, 80$, and failure percentages (FP) given by $\frac{v}{n} \times 100\% = 50\%$ and 75%. Additionally, for Set-1 and Set-2, the threshold values are set as $T = 2, 5$ and 0.5, 1.5, respectively.

To illustrate the effect of gamma and beta prior distributions on Bayesian estimation of the B12 parameters, historical sample data are used to determine suitable values for the hyper-parameters ξ_i and ζ_i ($i = 1, 2$) associated with σ and γ. A practical approach involves generating 10,000 complete datasets, each containing 50 observations, from a B12(σ, γ) distribution as historical reference samples for every possible estimate of the B12 parameters σ and γ. The resulting hyper-parameter values $(\xi_1, \xi_2, \zeta_1, \zeta_2)$ are then assigned as follows:

- For Set-1: (11.67946, 1.105608, 59.35436, 1.193479);
- For Set-2: (44.20721, 77.00427, 21.55486, 75.09214).

On the other hand, without loss of generality, the hyper-parameters ξ and ζ of p are chosen such that their prior expectation matches its true value; see also Kundu [22]. To compute Bayes point estimates along with 95% Bayesian credible intervals (BCIs) for σ, γ, $R(t)$, and $h(t)$, the proposed MCMC sampling procedure (detailed in Section 3) is carried out using $\mathcal{A} = 12{,}000$ and $\mathcal{A}^{\circ} = 2000$. Using the R software and two widely recommended packages—'maxLik' and 'coda' (Henningsen and Toomet [19] and Plummer et al. [21], respectively)—the point and interval estimates of σ, γ, $R(t)$, $h(t)$, and p are obtained. For the Markovian iterations, the initial values of the B12 parameters are set to their corresponding likelihood estimates.

For each scenario, the mean point estimate (MPE) of p (as an example) is determined as follows:

$$\text{MPE} = \frac{1}{1000} \sum\nolimits_{i=1}^{1000} \check{p}^{[i]},$$

where $\check{p}^{[i]}$ represents the estimated value of p from the ith sample.

To assess the accuracy of point estimates, two key metrics are utilized: root mean squared error (RMSE) and average relative absolute bias (ARAB), defined as follows:

$$\text{RMSE}\left(\check{p}\right) = \sqrt{\frac{1}{1000} \sum_{i=1}^{1000} \left(\check{p}^{[i]} - p\right)^2},$$

and

$$\text{ARAB}\left(\check{p}\right) = \frac{1}{1000} \sum_{i=1}^{1000} p^{-1} \left|\check{p}^{[i]} - p\right|.$$

For interval estimates, two additional precision measures are employed: the average interval length (AIL) and the coverage probability (CP), which are defined as follows:

$$\text{AIL}_{95\%}(p) = \frac{1}{1000} \sum_{i=1}^{1000} \left(\mathsf{U}_{\check{p}^{[i]}}(p) - \mathsf{L}_{\check{p}^{[i]}}(p)\right),$$

and

$$\mathrm{CP}_{95\%}(p) = \frac{1}{1000}\sum_{i=1}^{1000} \mathcal{O}_{\left(\mathsf{L}_{\tilde{p}^{[i]}}(p), \mathsf{U}_{\tilde{p}^{[i]}}(p)\right)}(p),$$

where $\mathcal{O}$ represents the indicator function, and $\mathsf{L}(\cdot)$, $\mathsf{U}(\cdot)$ correspond to the lower and upper bounds of the 95% confidence interval, respectively.

The MPE (1st column), RMSE (2nd column), and ARAB (3rd column) results for σ, γ, $R(t)$, $h(t)$, and p are presented in Tables 2–6, respectively. Additionally, Tables 7–11 report the AIL (1st column) and CP (2nd column) for σ, γ, $R(t)$, $h(t)$, and p, respectively.

From Tables 2–11, the following key conclusions are drawn by considering lower RMSE, ARAB, and AIL values, alongside higher CP values:

- The proposed estimation techniques provide reliable and consistent estimates for σ, γ, $R(t)$, $h(t)$, and p.
- Increasing n (or v) improves the precision of both point and interval estimates.
- Primarily due to the use of informative gamma and beta priors, the Bayes estimates and their corresponding credible interval estimates for σ, γ, $R(t)$, $h(t)$, and p exhibit superior accuracy compared to the frequentist estimates and asymptotic confidence interval estimates.
- As p increases, the following trends are observed across Set-1 and Set-2:
  - The RMSE, ARAB, and AIL values for σ, γ, and p decrease, while those for $R(t)$ and $h(t)$ increase.
  - The CP values for σ, γ, and p increase, whereas those for $R(t)$ and $h(t)$ decrease.
- As T increases, the following patterns emerge:
  - In Set-1: The RMSE, ARAB, and AIL values for σ, γ, $R(t)$, and $h(t)$ decrease, whereas the CP values exhibit the opposite trend.
  - In Set-2:
    - The RMSE and ARAB values of σ and $h(t)$ increase, while those of γ and $R(t)$ decrease.
    - The AIL values of σ, γ, $R(t)$, and $h(t)$ decrease, whereas the CP values show the opposite trend.
  - In both Set-1 and Set-2: The RMSE, ARAB, and AIL values of p decrease, whereas its CP values increase.
- As the B12(σ, γ) parameters increase:
  - The RMSE values of σ and $h(t)$ increase, while their corresponding ARAB values decrease.
  - The RMSE and ARAB values of γ and p decrease, whereas those of $R(t)$ increase.
  - The AIL values of γ and p decrease, while those of σ, $R(t)$, and $h(t)$ increase.
  - The CP values of γ and p increase, while those of σ, $R(t)$, and $h(t)$ decrease.
- Finally, based on the proposed censoring plan, the Bayesian framework incorporating the MCMC setup with independent gamma and beta priors is strongly recommended for analyzing lifetime data from a B12 distribution, particularly when one or more test units leave the experiment randomly according to a binomial probability law.

Table 2: The point estimation results of γ

p	FP [v]%		MLE			Bayes	
			Set-1				
				$T = 2$			
0.4	40 [50%]	0.371	0.191	0.860	0.254	0.140	0.298
	40 [75%]	0.246	0.146	0.636	0.230	0.090	0.267
	80 [50%]	0.263	0.090	0.382	0.215	0.076	0.242
	80 [75%]	0.224	0.087	0.351	0.222	0.063	0.226
0.8	40 [50%]	0.159	0.075	0.287	0.215	0.057	0.224
	40 [75%]	0.228	0.068	0.246	0.233	0.053	0.210
	80 [50%]	0.225	0.062	0.212	0.211	0.045	0.199
	80 [75%]	0.218	0.053	0.207	0.239	0.039	0.151
				$T = 5$			
0.4	40 [50%]	0.318	0.142	0.620	0.229	0.126	0.255
	40 [75%]	0.235	0.125	0.331	0.228	0.087	0.233
	80 [50%]	0.238	0.081	0.303	0.214	0.065	0.220
	80 [75%]	0.220	0.074	0.295	0.226	0.059	0.215
0.8	40 [50%]	0.249	0.072	0.289	0.154	0.052	0.201
	40 [75%]	0.226	0.065	0.240	0.225	0.049	0.191
	80 [50%]	0.220	0.059	0.204	0.206	0.041	0.179
	80 [75%]	0.217	0.051	0.193	0.241	0.033	0.145
			Set-2				
				$T = 0.5$			
0.4	40 [50%]	2.248	0.481	0.165	2.038	0.303	0.124
	40 [75%]	2.151	0.384	0.138	2.111	0.293	0.115
	80 [50%]	2.097	0.328	0.129	2.125	0.280	0.108
	80 [75%]	2.073	0.313	0.110	2.034	0.256	0.098
0.8	40 [50%]	2.134	0.271	0.102	2.185	0.235	0.099
	40 [75%]	2.075	0.228	0.099	2.137	0.214	0.094
	80 [50%]	2.055	0.206	0.088	2.108	0.180	0.068
	80 [75%]	2.040	0.186	0.074	2.007	0.175	0.067
				$T = 1.5$			
0.4	40 [50%]	2.313	0.626	0.220	2.034	0.320	0.129
	40 [75%]	2.183	0.533	0.187	2.160	0.298	0.120
	80 [50%]	2.139	0.374	0.138	2.135	0.278	0.110
	80 [75%]	2.106	0.372	0.140	2.070	0.266	0.106
0.8	40 [50%]	2.172	0.363	0.135	2.150	0.249	0.097
	40 [75%]	2.105	0.318	0.119	2.030	0.234	0.094
	80 [50%]	2.098	0.268	0.099	2.104	0.227	0.086
	80 [75%]	2.083	0.252	0.097	2.128	0.212	0.085

Table 3: The point estimation results of γ

p	FP [v]%	MLE			Bayes		
				Set-1			
				$T = 2$			
0.4	40 [50%]	0.519	0.507	0.400	0.689	0.296	0.324
	40 [75%]	0.820	0.451	0.377	0.629	0.258	0.277
	80 [50%]	0.738	0.421	0.344	0.852	0.232	0.218
	80 [75%]	0.895	0.332	0.311	0.694	0.204	0.201
0.8	40 [50%]	0.415	0.317	0.264	0.852	0.194	0.193
	40 [75%]	0.845	0.266	0.227	0.932	0.180	0.189
	80 [50%]	0.842	0.237	0.215	0.881	0.177	0.179
	80 [75%]	0.872	0.217	0.193	0.665	0.167	0.168
				$T = 5$			
0.4	40 [50%]	0.616	0.434	0.364	0.729	0.285	0.313
	40 [75%]	0.857	0.433	0.324	0.624	0.230	0.252
	80 [50%]	0.819	0.384	0.316	0.861	0.226	0.210
	80 [75%]	0.901	0.292	0.274	0.696	0.199	0.185
0.8	40 [50%]	0.764	0.262	0.223	1.265	0.184	0.180
	40 [75%]	0.835	0.249	0.202	0.892	0.179	0.177
	80 [50%]	0.844	0.218	0.194	0.871	0.167	0.170
	80 [75%]	0.852	0.199	0.189	0.699	0.153	0.159
				Set-2			
				$T = 0.5$			
0.4	40 [50%]	1.053	0.220	0.172	0.966	0.133	0.122
	40 [75%]	1.045	0.193	0.155	0.946	0.121	0.105
	80 [50%]	1.048	0.187	0.150	0.969	0.111	0.095
	80 [75%]	1.041	0.171	0.134	0.968	0.097	0.082
0.8	40 [50%]	1.032	0.142	0.127	1.104	0.094	0.076
	40 [75%]	1.040	0.132	0.110	1.007	0.090	0.073
	80 [50%]	1.035	0.120	0.103	0.974	0.078	0.061
	80 [75%]	1.033	0.119	0.095	0.899	0.072	0.058
				$T = 1.5$			
0.4	40 [50%]	1.036	0.190	0.158	1.104	0.128	0.118
	40 [75%]	1.028	0.188	0.148	0.951	0.118	0.096
	80 [50%]	1.039	0.170	0.131	0.970	0.104	0.086
	80 [75%]	1.029	0.169	0.128	0.968	0.092	0.078
0.8	40 [50%]	1.025	0.142	0.109	1.086	0.088	0.073
	40 [75%]	1.031	0.132	0.103	0.970	0.085	0.070
	80 [50%]	1.029	0.117	0.091	0.960	0.075	0.058
	80 [75%]	1.028	0.115	0.089	0.912	0.071	0.054

Table 4: The point estimation results of $R(t)$

p	FP [v]%		MLE			Bayes	
				Set-1			
				$T=2$			
0.4	40 [50%]	0.556	0.046	0.046	0.968	0.025	0.042
	40 [75%]	0.964	0.044	0.042	0.972	0.022	0.035
	80 [50%]	0.966	0.040	0.035	0.972	0.019	0.032
	80 [75%]	0.968	0.038	0.031	0.952	0.016	0.024
0.8	40 [50%]	0.898	0.096	0.090	0.951	0.060	0.077
	40 [75%]	0.955	0.087	0.076	0.949	0.047	0.064
	80 [50%]	0.948	0.062	0.069	0.968	0.039	0.056
	80 [75%]	0.964	0.058	0.057	0.957	0.029	0.046
				$T=5$			
0.4	40 [50%]	0.956	0.028	0.025	0.989	0.020	0.023
	40 [75%]	0.964	0.026	0.021	0.971	0.017	0.018
	80 [50%]	0.967	0.026	0.021	0.972	0.014	0.014
	80 [75%]	0.967	0.021	0.017	0.955	0.013	0.011
0.8	40 [50%]	0.923	0.062	0.058	0.958	0.053	0.052
	40 [75%]	0.958	0.052	0.042	0.949	0.044	0.041
	80 [50%]	0.958	0.040	0.035	0.969	0.035	0.033
	80 [75%]	0.964	0.032	0.029	0.957	0.028	0.025
				Set-2			
				$T=0.5$			
0.4	40 [50%]	0.823	0.056	0.049	0.846	0.040	0.041
	40 [75%]	0.830	0.047	0.047	0.817	0.037	0.038
	80 [50%]	0.831	0.042	0.043	0.807	0.035	0.035
	80 [75%]	0.831	0.040	0.039	0.787	0.033	0.033
0.8	40 [50%]	0.819	0.083	0.071	0.809	0.057	0.058
	40 [75%]	0.822	0.076	0.065	0.796	0.052	0.055
	80 [50%]	0.829	0.066	0.057	0.803	0.048	0.044
	80 [75%]	0.828	0.061	0.051	0.810	0.042	0.043
				$T=1.5$			
0.4	40 [50%]	0.818	0.053	0.042	0.842	0.039	0.038
	40 [75%]	0.825	0.042	0.043	0.812	0.036	0.036
	80 [50%]	0.826	0.038	0.040	0.802	0.034	0.034
	80 [75%]	0.826	0.032	0.038	0.781	0.031	0.031
0.8	40 [50%]	0.809	0.070	0.063	0.855	0.054	0.062
	40 [75%]	0.815	0.067	0.060	0.793	0.050	0.052
	80 [50%]	0.823	0.060	0.052	0.803	0.045	0.043
	80 [75%]	0.822	0.056	0.046	0.808	0.044	0.041

Table 5: The point estimation results of $h(t)$

p	FP $[v]$%	MLE			Bayes		
				Set-1			
				$T = 2$			
0.4	40 [50%]	0.181	0.107	0.407	0.226	0.075	0.259
	40 [75%]	0.244	0.091	0.346	0.229	0.071	0.236
	80 [50%]	0.240	0.085	0.318	0.217	0.067	0.214
	80 [75%]	0.228	0.080	0.301	0.279	0.060	0.204
0.8	40 [50%]	0.419	0.193	0.630	0.290	0.110	0.366
	40 [75%]	0.268	0.168	0.569	0.267	0.087	0.331
	80 [50%]	0.297	0.141	0.490	0.226	0.082	0.293
	80 [75%]	0.236	0.121	0.463	0.254	0.079	0.279
				$T = 5$			
0.4	40 [50%]	0.277	0.101	0.387	0.110	0.068	0.248
	40 [75%]	0.244	0.090	0.341	0.229	0.063	0.227
	80 [50%]	0.235	0.081	0.301	0.214	0.055	0.206
	80 [75%]	0.231	0.079	0.298	0.278	0.056	0.182
0.8	40 [50%]	0.364	0.157	0.525	0.257	0.104	0.355
	40 [75%]	0.254	0.138	0.455	0.265	0.081	0.304
	80 [50%]	0.261	0.119	0.423	0.224	0.078	0.281
	80 [75%]	0.233	0.108	0.415	0.259	0.073	0.268
				Set-2			
				$T = 0.5$			
0.4	40 [50%]	1.868	0.322	0.149	1.759	0.298	0.129
	40 [75%]	1.802	0.319	0.134	1.925	0.281	0.121
	80 [50%]	1.795	0.276	0.122	1.969	0.274	0.118
	80 [75%]	1.786	0.268	0.119	2.018	0.254	0.111
0.8	40 [50%]	1.911	0.465	0.299	1.919	0.365	0.216
	40 [75%]	1.849	0.448	0.230	2.024	0.344	0.185
	80 [50%]	1.805	0.387	0.182	1.992	0.324	0.156
	80 [75%]	1.799	0.375	0.164	1.909	0.313	0.148
				$T = 1.5$			
0.4	40 [50%]	1.913	0.366	0.169	1.771	0.301	0.130
	40 [75%]	1.844	0.353	0.155	1.903	0.298	0.128
	80 [50%]	1.844	0.325	0.143	1.994	0.262	0.121
	80 [75%]	1.834	0.301	0.132	2.114	0.256	0.111
0.8	40 [50%]	2.001	0.562	0.244	1.637	0.389	0.167
	40 [75%]	1.905	0.519	0.222	2.061	0.378	0.175
	80 [50%]	1.857	0.450	0.198	2.000	0.349	0.149
	80 [75%]	1.848	0.420	0.181	1.942	0.315	0.142

Table 6: The point estimation results of p

p	FP [v]%	MLE			Bayes		
				Set-1			
				$T = 2$			
0.4	40 [50%]	0.408	0.113	0.205	0.405	0.092	0.140
	40 [75%]	0.806	0.108	0.179	0.803	0.086	0.129
	80 [50%]	0.417	0.107	0.159	0.408	0.079	0.118
	80 [75%]	0.815	0.088	0.145	0.805	0.069	0.088
0.8	40 [50%]	0.239	0.079	0.121	0.403	0.063	0.076
	40 [75%]	0.803	0.076	0.092	0.802	0.056	0.062
	80 [50%]	0.412	0.073	0.088	0.408	0.046	0.056
	80 [75%]	0.808	0.056	0.056	0.804	0.042	0.047
				$T = 5$			
0.4	40 [50%]	0.409	0.111	0.184	0.406	0.087	0.139
	40 [75%]	0.806	0.106	0.145	0.803	0.082	0.124
	80 [50%]	0.420	0.102	0.135	0.409	0.066	0.118
	80 [75%]	0.815	0.083	0.111	0.805	0.062	0.088
0.8	40 [50%]	0.407	0.076	0.097	0.406	0.059	0.066
	40 [75%]	0.803	0.073	0.079	0.802	0.056	0.062
	80 [50%]	0.413	0.059	0.070	0.409	0.049	0.056
	80 [75%]	0.808	0.050	0.056	0.804	0.045	0.048
				Set-2			
				$T = 0.5$			
0.4	40 [50%]	0.415	0.107	0.202	0.410	0.082	0.136
	40 [75%]	0.806	0.105	0.151	0.803	0.076	0.124
	80 [50%]	0.421	0.080	0.143	0.410	0.070	0.113
	80 [75%]	0.815	0.079	0.111	0.805	0.064	0.083
0.8	40 [50%]	0.407	0.079	0.097	0.406	0.059	0.072
	40 [75%]	0.803	0.073	0.079	0.802	0.054	0.061
	80 [50%]	0.413	0.056	0.078	0.409	0.044	0.052
	80 [75%]	0.808	0.050	0.056	0.804	0.039	0.047
				$T = 1.5$			
0.4	40 [50%]	0.405	0.109	0.202	0.402	0.077	0.134
	40 [75%]	0.794	0.105	0.149	0.793	0.070	0.120
	80 [50%]	0.421	0.101	0.143	0.410	0.062	0.112
	80 [75%]	0.813	0.079	0.112	0.804	0.061	0.076
0.8	40 [50%]	0.407	0.075	0.097	0.406	0.057	0.062
	40 [75%]	0.802	0.073	0.091	0.801	0.052	0.056
	80 [50%]	0.413	0.058	0.078	0.409	0.041	0.047
	80 [75%]	0.808	0.050	0.057	0.804	0.034	0.041

Table 7: The interval estimation results of σ

p	FP [v]%	ACI		BCI		ACI		BCI	
					Set-1				
$T \rightarrow$				2				5	
0.4	40 [50%]	0.387	0.941	0.276	0.945	0.375	0.943	0.219	0.947
	40 [75%]	0.349	0.943	0.240	0.946	0.331	0.945	0.190	0.948
	80 [50%]	0.315	0.945	0.219	0.948	0.295	0.947	0.184	0.949
	80 [75%]	0.287	0.946	0.199	0.950	0.283	0.949	0.177	0.952
0.8	40 [50%]	0.231	0.949	0.186	0.952	0.225	0.951	0.166	0.954
	40 [75%]	0.216	0.950	0.176	0.953	0.203	0.952	0.158	0.954
	80 [50%]	0.199	0.951	0.161	0.955	0.197	0.953	0.147	0.956
	80 [75%]	0.186	0.952	0.144	0.957	0.178	0.953	0.135	0.958
					Set-2				
$T \rightarrow$		0.5				1.5			
0.4	40 [50%]	2.017	0.917	1.353	0.929	1.966	0.980	1.257	0.931
	40 [75%]	1.907	0.918	1.238	0.932	1.795	0.981	1.121	0.933
	80 [50%]	1.585	0.922	1.091	0.935	1.545	0.984	1.008	0.935
	80 [75%]	1.490	0.925	0.982	0.937	1.459	0.984	0.911	0.938
0.8	40 [50%]	1.334	0.927	0.910	0.939	1.236	0.985	0.891	0.941
	40 [75%]	1.291	0.930	0.887	0.941	1.136	0.985	0.821	0.941
	80 [50%]	1.142	0.933	0.785	0.942	1.067	0.987	0.768	0.943
	80 [75%]	1.034	0.935	0.738	0.943	0.995	0.988	0.719	0.944

Table 8: The interval estimation results of γ

p	FP [v]%	ACI		BCI		ACI		BCI	
					Set-1				
$T \rightarrow$				2				5	
0.4	40 [50%]	1.231	0.916	1.073	0.920	1.216	0.918	0.836	0.923
	40 [75%]	1.155	0.918	0.832	0.924	1.136	0.920	0.784	0.926
	80 [50%]	0.941	0.921	0.784	0.927	0.936	0.923	0.654	0.929
	80 [75%]	0.852	0.924	0.696	0.929	0.833	0.926	0.616	0.930
0.8	40 [50%]	0.789	0.927	0.614	0.931	0.777	0.929	0.583	0.932
	40 [75%]	0.735	0.929	0.596	0.932	0.720	0.931	0.528	0.934
	80 [50%]	0.672	0.932	0.529	0.936	0.627	0.934	0.476	0.938
	80 [75%]	0.616	0.933	0.457	0.938	0.587	0.935	0.443	0.939

(Continued)

Table 8 **(continued)**

p	FP [v]%	ACI		BCI		ACI		BCI	
Set-2									
$T \to$		0.5				1.5			
0.4	40 [50%]	0.670	0.937	0.612	0.937	0.643	0.903	0.589	0.939
	40 [75%]	0.629	0.938	0.577	0.939	0.613	0.909	0.542	0.940
	80 [50%]	0.576	0.940	0.537	0.941	0.549	0.916	0.477	0.943
	80 [75%]	0.533	0.941	0.465	0.943	0.514	0.918	0.393	0.945
0.8	40 [50%]	0.477	0.944	0.375	0.945	0.458	0.921	0.352	0.947
	40 [75%]	0.423	0.945	0.325	0.946	0.414	0.922	0.313	0.948
	80 [50%]	0.398	0.946	0.296	0.948	0.382	0.926	0.263	0.950
	80 [75%]	0.368	0.947	0.262	0.949	0.356	0.929	0.246	0.951

Table 9: The interval estimation results of $R(t)$

p	FP [v]%	ACI		BCI		ACI		BCI	
Set-1									
$T \to$		2				5			
0.4	40 [50%]	0.088	0.940	0.077	0.941	0.077	0.941	0.072	0.941
	40 [75%]	0.077	0.941	0.067	0.942	0.070	0.941	0.064	0.942
	80 [50%]	0.068	0.942	0.055	0.943	0.063	0.942	0.051	0.944
	80 [75%]	0.062	0.942	0.048	0.943	0.052	0.943	0.041	0.945
0.8	40 [50%]	0.181	0.933	0.124	0.935	0.162	0.934	0.113	0.938
	40 [75%]	0.153	0.935	0.114	0.937	0.133	0.936	0.108	0.939
	80 [50%]	0.133	0.936	0.091	0.939	0.122	0.937	0.087	0.940
	80 [75%]	0.110	0.938	0.083	0.939	0.096	0.940	0.078	0.941
Set-2									
$T \to$		0.5				1.5			
0.4	40 [50%]	0.175	0.933	0.167	0.935	0.167	0.934	0.145	0.936
	40 [75%]	0.167	0.935	0.133	0.937	0.160	0.936	0.122	0.938
	80 [50%]	0.150	0.937	0.121	0.939	0.147	0.938	0.112	0.940
	80 [75%]	0.140	0.938	0.111	0.940	0.132	0.939	0.106	0.941
0.8	40 [50%]	0.264	0.928	0.225	0.930	0.243	0.929	0.195	0.931
	40 [75%]	0.233	0.930	0.215	0.931	0.224	0.931	0.185	0.932
	80 [50%]	0.219	0.931	0.195	0.932	0.211	0.932	0.166	0.934
	80 [75%]	0.210	0.931	0.177	0.934	0.207	0.932	0.159	0.935

Table 10: The interval estimation results of $h(t)$

p	FP $[v]$%	ACI		BCI		ACI		BCI	
				Set-1					
$T \rightarrow$			2				5		
0.4	40 [50%]	0.384	0.945	0.274	0.949	0.359	0.947	0.242	0.951
	40 [75%]	0.359	0.947	0.252	0.950	0.334	0.949	0.238	0.952
	80 [50%]	0.310	0.950	0.230	0.952	0.289	0.952	0.228	0.954
	80 [75%]	0.286	0.952	0.221	0.953	0.268	0.954	0.217	0.955
0.8	40 [50%]	0.565	0.936	0.397	0.940	0.512	0.938	0.378	0.942
	40 [75%]	0.482	0.940	0.363	0.942	0.464	0.942	0.327	0.944
	80 [50%]	0.478	0.942	0.327	0.945	0.435	0.944	0.296	0.947
	80 [75%]	0.421	0.943	0.296	0.947	0.403	0.945	0.264	0.949
				Set-2					
$T \rightarrow$			0.5				1.5		
0.4	40 [50%]	1.482	0.933	1.013	0.939	1.432	0.934	0.994	0.937
	40 [75%]	1.387	0.935	0.976	0.940	1.332	0.936	0.888	0.940
	80 [50%]	1.236	0.938	0.933	0.941	1.214	0.939	0.850	0.941
	80 [75%]	1.118	0.940	0.891	0.943	1.096	0.941	0.794	0.943
0.8	40 [50%]	1.995	0.922	1.741	0.929	1.855	0.924	1.190	0.935
	40 [75%]	1.889	0.924	1.487	0.932	1.719	0.926	1.185	0.935
	80 [50%]	1.707	0.927	1.216	0.936	1.686	0.928	1.073	0.936
	80 [75%]	1.659	0.930	1.055	0.938	1.579	0.931	1.002	0.936

Table 11: The interval estimation results of p

p	FP $[v]$%	ACI		BCI		ACI		BCI	
				Set-1					
$T \rightarrow$			2				5		
0.4	40 [50%]	0.424	0.937	0.334	0.942	0.412	0.938	0.324	0.943
	40 [75%]	0.398	0.939	0.319	0.943	0.389	0.940	0.296	0.945
	80 [50%]	0.331	0.942	0.275	0.945	0.323	0.944	0.261	0.947
	80 [75%]	0.299	0.945	0.262	0.946	0.272	0.946	0.254	0.947
0.8	40 [50%]	0.288	0.946	0.236	0.948	0.269	0.947	0.224	0.949
	40 [75%]	0.274	0.947	0.229	0.950	0.254	0.948	0.201	0.952
	80 [50%]	0.236	0.949	0.201	0.951	0.216	0.950	0.190	0.952
	80 [75%]	0.214	0.950	0.194	0.952	0.193	0.951	0.176	0.953

(Continued)

Table 11 (continued)

p	FP [v]%	ACI		BCI		ACI		BCI	
				Set-2					
$T \to$			0.5				1.5		
0.4	40 [50%]	0.422	0.925	0.323	0.944	0.409	0.915	0.317	0.943
	40 [75%]	0.386	0.933	0.286	0.946	0.369	0.903	0.274	0.947
	80 [50%]	0.330	0.947	0.272	0.947	0.318	0.946	0.261	0.948
	80 [75%]	0.292	0.896	0.255	0.948	0.269	0.892	0.245	0.947
0.8	40 [50%]	0.274	0.946	0.227	0.950	0.261	0.945	0.213	0.951
	40 [75%]	0.258	0.950	0.200	0.952	0.247	0.948	0.198	0.952
	80 [50%]	0.222	0.953	0.194	0.952	0.211	0.953	0.183	0.953
	80 [75%]	0.193	0.929	0.157	0.954	0.179	0.929	0.146	0.955

6 Fibers Data Analysis

To assess the applicability and significance of the proposed estimation methodologies in real-world scenarios, two separate genuine datasets from physical experiments are analyzed.

6.1 Polyester Fiber

Polyester fibers are highly durable, wrinkle-resistant, quick-drying, and retain their shape, making them ideal for long-lasting, low-maintenance fabrics. From a physics perspective, these fibers are advantageous due to their high tensile strength, thermal stability, and insulating properties, which make them suitable for applications such as composites, insulation, and materials for experimental apparatuses. In this study, we analyze a dataset containing thirty measurements of the tensile strength of polyester fibers (see Table 12). This dataset was later revisited by Irfan et al. [23].

Table 12: Tensile strength of polyester fibers

0.023	0.032	0.054	0.069	0.081	0.094	0.105	0.127	0.148	0.169
0.188	0.216	0.255	0.277	0.311	0.361	0.376	0.395	0.432	0.463
0.481	0.519	0.529	0.567	0.642	0.674	0.752	0.823	0.887	0.926

First, before evaluating the proposed inferential methodologies, the suitability of the B12 model for the polyester fibers dataset presented in Table 12 was examined. This assessment was performed using the Kolmogorov–Smirnov (KS) test and its corresponding p-value. Additionally, the MLEs of the B12 parameters σ and γ, along with their respective standard errors (SErrs) and 95% ACIs (including interval widths, IWs), were obtained (see Table 13). The results in Table 13 indicate that the B12 lifetime distribution provides an excellent fit to the polyester fibers dataset. Fig. 2 presents five graphical evaluations: (a) probability–probability (PP) plot; (b) quantile–quantile (QQ) plot; (c) scaled total time on test (TTT) plot; (d) empirical and fitted reliability lines $R(x)$; and (e) contour plot of the parameter estimates.

Table 13: Fit results of B12 model from polyester fibers data

Par.	MLE		95% ACI			*KS*	
	Est.	SErr	Low.	Upp.	IW	Distance	p-value
σ	4.5067	0.9691	2.6074	6.4061	3.7987	0.1036	0.8713
γ	1.4512	0.2013	1.0566	1.8458	0.7892		

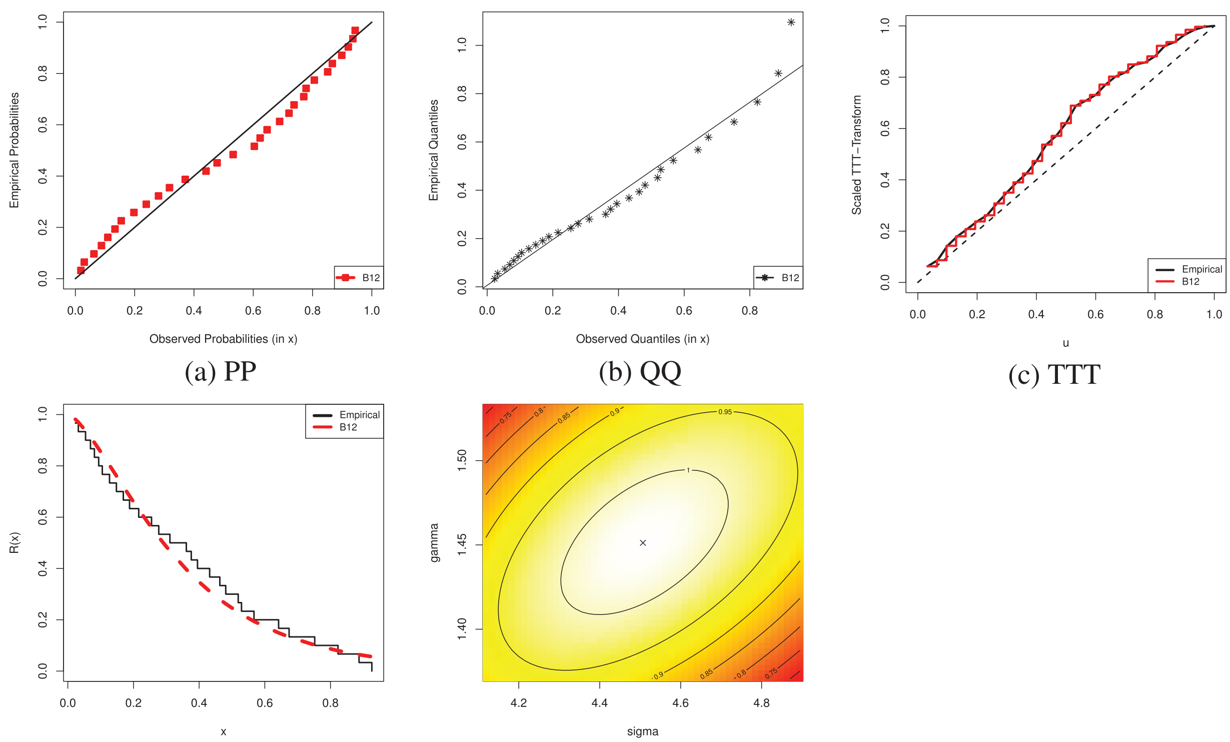

(a) PP (b) QQ (c) TTT

(d) RF (e) Contour

Figure 2: Five fitting representations for B12 model from polyester fibers data (a–e)

The visual analysis in Fig. 2a–d reinforces the conclusion that the B12 model effectively captures the underlying characteristics of the observed polyester fibers data, in agreement with the results shown in Table 13. Fig. 2c further indicates that the polyester fibers data exhibit an increasing failure rate, consistent with the theoretical hazard function of the B12 model. Additionally, Fig. 2d confirms the existence and uniqueness of the calculated MLEs $\hat{\sigma}$ and $\hat{\gamma}$ of σ and γ, respectively. This demonstrates that the obtained estimates exist and are unique; consequently, these estimates are recommended as initial values for future computational procedures to enhance numerical stability and precision. From the complete polyester fibers dataset reported in Table 12, six APH-CSBR-TII samples are generated under varying design configurations of p, T, and v (see Table 14). Assuming non-informative priors for the B12 and binomial parameters, improper gamma and beta prior distributions are employed for (σ, γ) and p, respectively.

Table 14: Six APH-CSBR-TII samples from polyester fibers data

Sample		$(p, v) = (0.3, 10)$ and $\{T(d), r^*\} = \{0.12(3), 7\}$									
S1	i	1	2	3	4	5	6	7	8	9	10
	r_i	4	5	4	0	0	0	0	0	0	0
	x_i	0.023	0.054	0.094	0.148	0.216	0.311	0.395	0.463	0.519	0.642
		$(p, v) = (0.6, 10)$ and $\{T(d), r^*\} = \{0.07(2), 2\}$									
S2	i	1	2	3	4	5	6	7	8	9	10
	r_i	15	3	0	0	0	0	0	0	0	0
	x_i	0.023	0.069	0.081	0.127	0.188	0.277	0.376	0.432	0.481	0.567
		$(p, v) = (0.9, 10)$ and $\{T(d), r^*\} = \{0.05(1), 1\}$									
S3	i	1	2	3	4	5	6	7	8	9	10
	r_i	19	0	0	0	0	0	0	0	0	0
	x_i	0.023	0.081	0.105	0.169	0.255	0.311	0.361	0.395	0.463	0.519
		$(p, v) = (0.3, 20)$ and $\{T(d), r^*\} = \{0.07(3), 4\}$									
S4	i	1	2	3	4	5	6	7	8	9	10
	r_i	1	3	2	0	0	0	0	0	0	0
	x_i	0.023	0.032	0.069	0.081	0.094	0.105	0.127	0.169	0.188	0.216
	i	11	12	13	14	15	16	17	18	19	20
	r_i	0	0	0	0	0	0	0	0	0	0
	x_i	0.277	0.376	0.395	0.432	0.463	0.519	0.567	0.642	0.674	0.752
		$(p, v) = (0.6, 20)$ and $\{T(d), r^*\} = \{0.06(2), 1\}$									
S5	i	1	2	3	4	5	6	7	8	9	10
	r_i	8	1	0	0	0	0	0	0	0	0
	x_i	0.023	0.054	0.069	0.094	0.105	0.127	0.148	0.188	0.255	0.311
	i	11	12	13	14	15	16	17	18	19	20
	r_i	0	0	0	0	0	0	0	0	0	0
	x_i	0.361	0.376	0.395	0.432	0.463	0.481	0.519	0.529	0.567	0.674
		$(p, v) = (0.9, 20)$ and $\{T(d), r^*\} = \{0.03(1), 1\}$									
S6	i	1	2	3	4	5	6	7	8	9	10
	r_i	9	0	0	0	0	0	0	0	0	0
	x_i	0.023	0.054	0.069	0.081	0.094	0.148	0.169	0.216	0.255	0.277
	i	11	12	13	14	15	16	17	18	19	20
	r_i	0	0	0	0	0	0	0	0	0	0
	x_i	0.311	0.361	0.376	0.395	0.432	0.463	0.481	0.519	0.567	0.642

From the complete polyester fibers dataset reported in Table 12, six APH-CSBR-TII samples are generated under varying design configurations of p, T, and v (see Table 14). Assuming non-informative priors for the B12 and binomial parameters, improper gamma and beta prior distributions are employed for (σ, γ) and p, respectively. A total of $\mathcal{T} = 40{,}000$ MCMC iterations, including a burn-in phase of $\mathcal{T}^{\circ} = 10{,}000$ iterations, are conducted to obtain Bayesian point estimates and 95% BCI bounds for σ, γ, $R(t)$, $h(t)$, and p. For S_i, $i = 1, 2, \ldots, 6$ (Table 14), the maximum likelihood and Bayesian MCMC estimates (along with their SErrs) of σ, γ, $R(t)$ (at $t = 0.15$), $h(t)$ (at $t = 0.15$), and p are calculated (see Table 15). Additionally, Table 15 presents the corresponding 95% ACIs/BCIs, along with their interval lengths (ILs), for these parameters. The results in Table 15 demonstrate that the Bayesian estimators for σ, γ, $R(t)$, $h(t)$, and p exhibit improved performance over the likelihood-based estimates, as reflected by their reduced SErr values. Moreover, the BCIs provide a clear advantage over the ACIs due to their shorter ILs, confirming their higher estimation efficiency.

Table 15: Point and interval estimates of σ, γ, $R(t)$, $h(t)$, and p from polyester fibers data

(p, v)	Par.	MLE		Bayes		ACI			BCI		
		Est.	SErr	Est.	SErr	Low.	Upp.	IL	Low.	Upp.	IL
S1	σ	1.8140	0.6734	1.8001	0.1464	0.4941	3.1338	2.6398	1.5140	2.0889	0.5749
	γ	1.2411	0.2850	1.2315	0.1278	0.6825	1.7997	1.1172	0.9860	1.4859	0.4999
	$R(0.15)$	0.7418	0.0796	0.7393	0.0394	0.5858	0.8979	0.3121	0.6575	0.8107	0.1532
	$h(0.15)$	1.3670	0.4493	1.3524	0.1233	0.4865	2.2475	1.7611	1.1148	1.5926	0.4778
	p	0.2766	0.0652	0.2776	0.0686	0.1487	0.4045	0.2558	0.1610	0.4132	0.2522
S2	σ	4.2593	1.7577	4.2516	0.1487	0.8143	7.7044	6.8901	3.9614	4.5454	0.5840
	γ	1.4360	0.3010	1.4272	0.1262	0.8460	2.0260	1.1800	1.1881	1.6804	0.4923
	$R(0.15)$	0.5796	0.1076	0.5751	0.0524	0.3688	0.7905	0.4217	0.4710	0.6756	0.2046
	$h(0.15)$	2.9403	0.9818	2.9380	0.2104	1.0160	4.8645	3.8485	2.5032	3.3288	0.8256
	p	0.7200	0.0898	0.7178	0.1470	0.5440	0.8960	0.3520	0.5306	0.8714	0.3408
S3	σ	6.5022	2.9041	6.4963	0.1491	0.8104	12.194	11.384	6.2054	6.7908	0.5854
	γ	1.6684	0.3596	1.6599	0.1292	0.9637	2.3731	1.4095	1.4136	1.9188	0.5052
	$R(0.15)$	0.5414	0.1161	0.5364	0.0568	0.3138	0.7689	0.4551	0.4238	0.6456	0.2217
	$h(0.15)$	3.9081	1.2616	3.9229	0.3375	1.4354	6.3807	4.9452	3.2440	4.5667	1.3227
	p	0.7500	0.0487	0.9455	0.0669	0.5448	0.8946	0.3497	0.8162	0.9980	0.1818
S4	σ	3.1175	0.8021	3.1082	0.1469	1.5454	4.6896	3.1442	2.8216	3.3975	0.5759
	γ	1.2573	0.2093	1.2490	0.1166	0.8471	1.6675	0.8204	1.0265	1.4815	0.4550
	$R(0.15)$	0.6049	0.0803	0.6014	0.0465	0.4476	0.7622	0.3146	0.5087	0.6902	0.1815
	$h(0.15)$	2.3350	0.5332	2.3233	0.1447	1.2899	3.3802	2.0902	2.0295	2.5986	0.5691
	p	0.2400	0.0854	0.2422	0.1015	0.0726	0.4074	0.3348	0.1002	0.4235	0.3233
S5	σ	5.4518	1.6282	5.4452	0.1486	2.2606	8.6430	6.3824	5.1552	5.7388	0.5837
	γ	1.5867	0.2669	1.5790	0.1207	1.0635	2.1099	1.0464	1.3485	1.8204	0.4720
	$R(0.15)$	0.5638	0.0880	0.5595	0.0515	0.3913	0.7362	0.3449	0.4570	0.6584	0.2014
	$h(0.15)$	3.4526	0.7828	3.4594	0.2648	1.9184	4.9869	3.0685	2.9245	3.9614	1.0368
	p	0.7500	0.1250	0.7456	0.1884	0.5050	0.9950	0.4900	0.4784	0.9360	0.4575
S6	σ	5.9370	1.8088	5.9307	0.1488	2.3919	9.4821	7.0903	5.6401	6.2246	0.5845

(Continued)

Table 15 (continued)

(p, v)	Par.	MLE		Bayes		ACI			BCI		
		Est.	SErr	Est.	SErr	Low.	Upp.	IL	Low.	Upp.	IL
	γ	1.6169	0.2706	1.6094	0.1201	1.0866	2.1472	1.0606	1.3797	1.8498	0.4701
	$R(0.15)$	0.5490	0.0883	0.5447	0.0522	0.3759	0.7220	0.3460	0.4413	0.6452	0.2040
	$h(0.15)$	3.6894	0.8330	3.6984	0.2867	2.0569	5.3220	3.2652	3.1214	4.2435	1.1221
	p	0.9000	0.0949	0.8921	0.0926	0.7141	0.9939	0.2798	0.6537	0.9959	0.3421

Using S_i, $i = 1, 2, \ldots, 6$ (Table 14), Fig. 3 displays the estimated profile log-likelihood curves for σ and γ. These curves confirm the existence and uniqueness of the MLEs, $\hat{\sigma}$ and $\hat{\gamma}$, thereby supporting the fitted values presented in Table 15. Trace plots and density plots are standard MCMC diagnostic tools: trace plots assess how well the chain explores the posterior distribution, while density plots illustrate the posterior distribution itself, providing additional confidence in the validity of the Bayesian estimates. Considering S_1 (from Table 14) as a representative sample, Fig. 4 presents the density and trace plots for σ, γ, $R(t)$, $h(t)$, and p, generated from 30,000 MCMC iterations. These visualizations indicate that the simulated Markov chains achieve satisfactory convergence and that the designated burn-in period of 10,000 iterations effectively mitigates the influence of initial values; see, for more details, Kavianihamedani et al. [24]. Furthermore, the posterior distributions based on the 30,000 retained iterations exhibit reasonable symmetry for σ, γ, and p; positive skewness for $h(t)$; and negative skewness for $R(t)$.

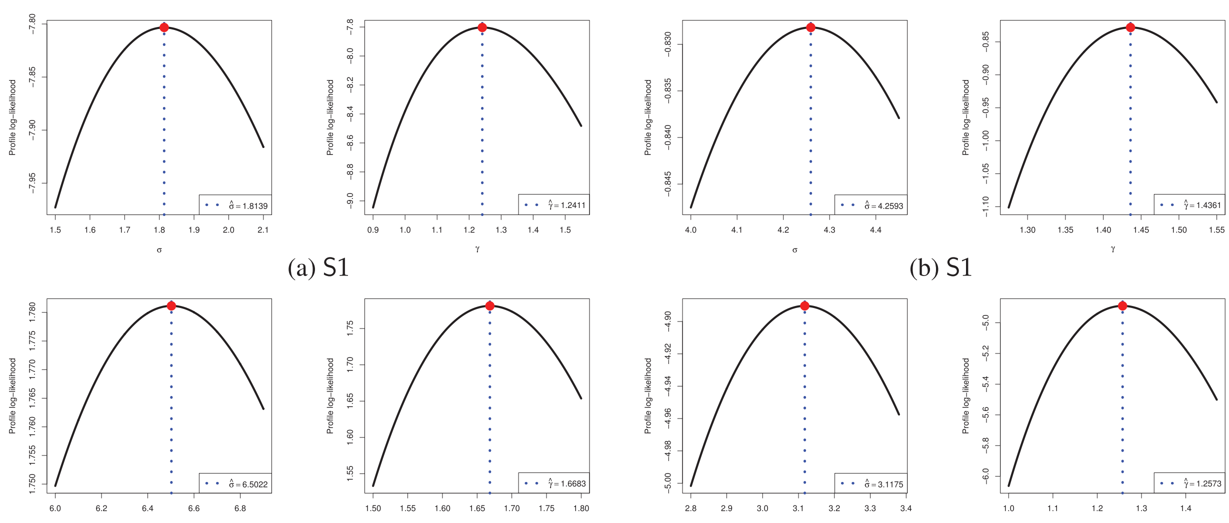

(a) S1 (b) S1

(c) S1 (d) S1

Figure 3: (Continued)

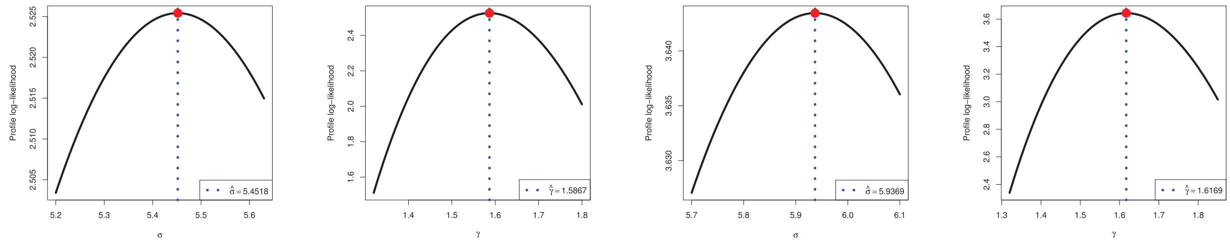

(e) S1 (f) S1

Figure 3: Profile log-likelihood curves of σ (left) and γ (right) from polyester fibers data (a–f)

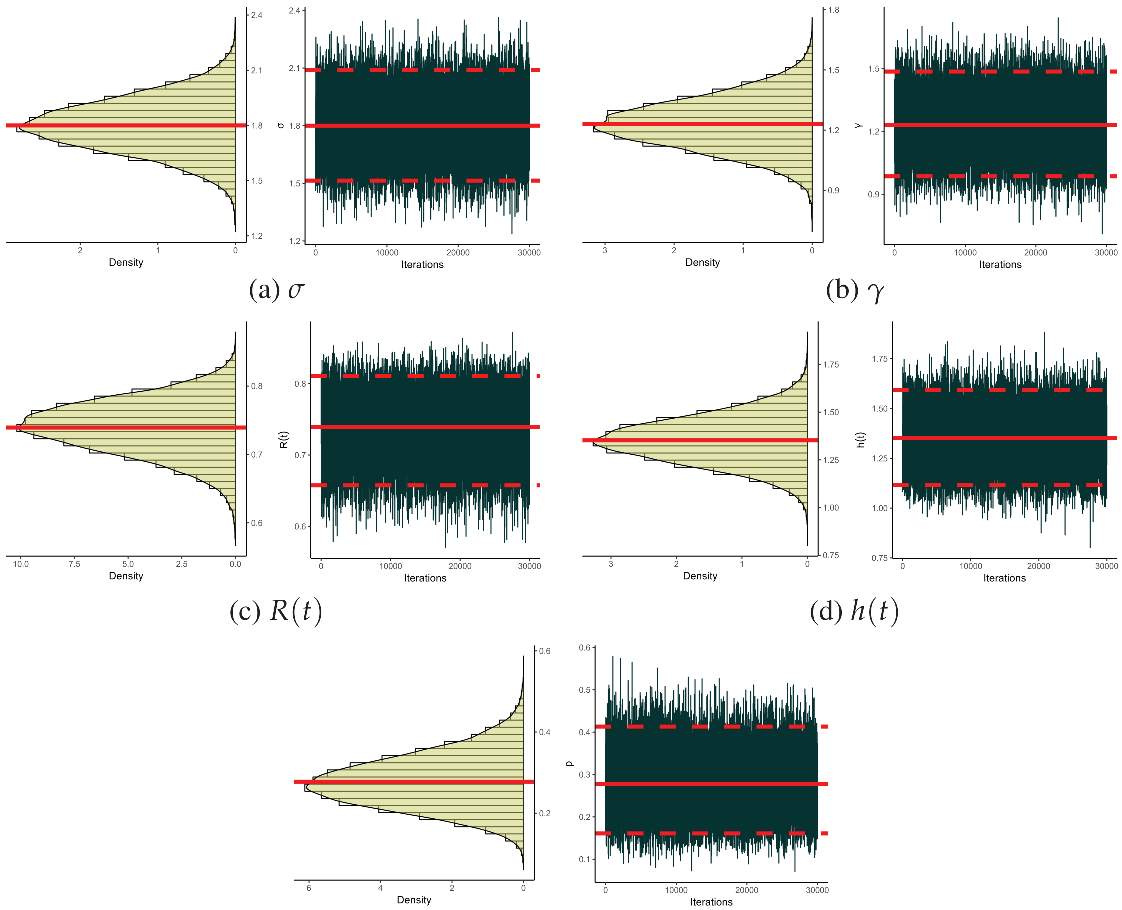

(a) σ (b) γ (c) $R(t)$ (d) $h(t)$ (e) p

Figure 4: The density and trace plots of (a): σ, (b): γ, (c): $R(t)$, (d): $h(t)$, and (e): p from polyester fibers data

The results obtained from the polyester fibers dataset, using an adaptive Type-II progressively censoring mechanism with binomial random removals, underscore the practical significance and real-world applicability of the proposed methodologies.

6.2 Carbon Fiber

Carbon fibers are lightweight yet exceptionally strong and rigid, providing high durability, thermal resistance, and excellent conductivity, making them ideal for aerospace, automotive, and structural applications. In this study, using the dataset from Nichols and Padgett [25], we analyze the breaking stress of carbon fibers (in giga-Pascals, GPa). For computational convenience, each breaking stress value is divided by ten, and the resulting dataset is presented in Table 16. The model fit results in Table 17 confirm that the B12 distribution provides an excellent representation of the complete carbon fiber dataset.

Table 16: Breaking stress of 66 carbon fibers

0.039	0.085	0.108	0.125	0.147	0.157	0.161	0.161	0.169	0.180
0.184	0.187	0.189	0.203	0.203	0.205	0.212	0.235	0.241	0.243
0.248	0.250	0.253	0.255	0.255	0.256	0.259	0.267	0.273	0.274
0.279	0.281	0.282	0.285	0.287	0.288	0.293	0.295	0.296	0.297
0.309	0.311	0.311	0.315	0.315	0.319	0.322	0.322	0.327	0.328
0.331	0.331	0.333	0.339	0.339	0.356	0.360	0.365	0.368	0.370
0.375	0.420	0.438	0.442	0.470	0.490				

Table 17: Fit results of B12 model from carbon fibers data

Par.	MLE		95% ACI			*KS*	
	Est.	SErr	Low.	Upp.	IW	Distance	p-value
σ	62.028	22.441	18.368	103.09	84.725	0.0829	0.7544
γ	3.4779	0.3236	2.8368	4.0852	1.2484		

Fig. 5a–b illustrates the fitting results summarized in Table 17. Additionally, Fig. 5c shows that the ARTs dataset exhibits an increasing trend, consistent with one of the theoretical failure rate shapes of the IW distribution. Furthermore, Fig. 5d confirms the existence and uniqueness of the estimated parameters $\hat{\sigma}$ and $\hat{\gamma}$ derived from the ARTs dataset. Consequently, these parameter estimates are recommended as initial values in future computational procedures to improve numerical accuracy and efficiency.

Using the complete carbon fiber dataset, six APH-CSBR-TII samples are generated with varying values of p, T, and v (see Table 18). Following the MCMC setup described in Section 6.1, the Bayesian point estimates and 95% BCI estimates of σ, γ, $R(t)$, $h(t)$, and p are calculated (see Table 19). The same table also presents the MLEs and their corresponding 95% ACI estimates for each unknown parameter. Considering the lower SErr and IL values, Table 19 indicates that the Bayesian estimates (along with their BCIs) of σ, γ, $R(t)$, $h(t)$, and p outperform the likelihood estimates (and their ACIs).

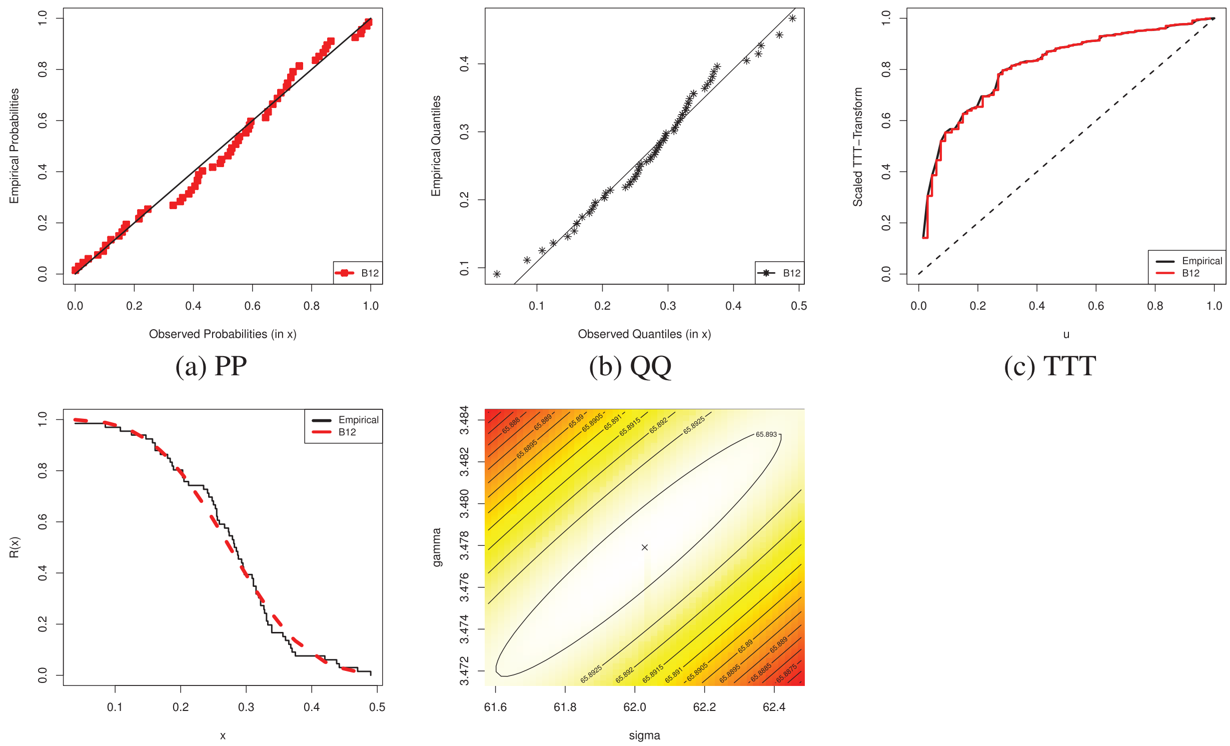

(a) PP (b) QQ (c) TTT

(d) RF (e) Contour

Figure 5: Five fitting representations for B12 model from carbon fibers data (a–e)

Table 18: Six APH-CSBR-TII samples from carbon fibers data

Sample	$(p, v) = (0.3, 10)$ and $\{T(d), r^*\} = \{0.17(4), 13\}$										
S1	i	1	2	3	4	5	6	7	8	9	10
	r_i	13	14	9	7	0	0	0	0	0	0
	x_i	0.039	0.108	0.125	0.161	0.203	0.255	0.293	0.322	0.360	0.438

	$(p, v) = (0.6, 10)$ and $\{T(d), r^*\} = \{0.15(3), 4\}$										
S2	i	1	2	3	4	5	6	7	8	9	10
	r_i	38	10	4	0	0	0	0	0	0	0
	x_i	0.039	0.085	0.147	0.169	0.205	0.259	0.296	0.328	0.365	0.420

	$(p, v) = (0.9, 10)$ and $\{T(d), r^*\} = \{0.05(1), 3\}$										
S3	i	1	2	3	4	5	6	7	8	9	10
	r_i	53	0	0	0	0	0	0	0	0	0
	x_i	0.039	0.108	0.147	0.161	0.189	0.241	0.279	0.315	0.356	0.375

(Continued)

Table 18 (continued)

		$(p, v) = (0.3, 30)$ and $\{T(d), r^*\} = \{0.17(5), 5\}$									
S4	i	1	2	3	4	5	6	7	8	9	10
	r_i	8	9	6	4	4	0	0	0	0	0
	x_i	0.039	0.085	0.147	0.157	0.169	0.180	0.187	0.189	0.203	0.235
	i	11	12	13	14	15	16	17	18	19	20
	r_i	0	0	0	0	0	0	0	0	0	0
	x_i	0.241	0.243	0.250	0.253	0.255	0.267	0.273	0.281	0.288	0.293
	i	21	22	23	24	25	26	27	28	29	30
	r_i	0	0	0	0	0	0	0	0	0	0
	x_i	0.297	0.309	0.319	0.327	0.339	0.360	0.368	0.375	0.420	0.442
		$(p, v) = (0.6, 30)$ and $\{T(d), r^*\} = \{0.13(3), 2\}$									
S5	i	1	2	3	4	5	6	7	8	9	10
	r_i	25	6	3	0	0	0	0	0	0	0
	x_i	0.039	0.108	0.125	0.157	0.169	0.187	0.205	0.241	0.250	0.259
	i	11	12	13	14	15	16	17	18	19	20
	r_i	0	0	0	0	0	0	0	0	0	0
	x_i	0.267	0.274	0.279	0.281	0.287	0.293	0.295	0.297	0.309	0.311
	i	21	22	23	24	25	26	27	28	29	30
	r_i	0	0	0	0	0	0	0	0	0	0
	x_i	0.315	0.322	0.328	0.331	0.339	0.339	0.360	0.370	0.375	0.420
		$(p, v) = (0.9, 30)$ and $\{T(d), r^*\} = \{0.04(1), 2\}$									
S6	i	1	2	3	4	5	6	7	8	9	10
	r_i	34	0	0	0	0	0	0	0	0	0
	x_i	0.039	0.085	0.147	0.157	0.169	0.187	0.189	0.205	0.212	0.235
	i	11	12	13	14	15	16	17	18	19	20
	r_i	0	0	0	0	0	0	0	0	0	0
	x_i	0.241	0.243	0.250	0.255	0.267	0.273	0.279	0.285	0.288	0.293
	i	21	22	23	24	25	26	27	28	29	30
	r_i	0	0	0	0	0	0	0	0	0	0
	x_i	0.297	0.309	0.311	0.319	0.328	0.339	0.356	0.365	0.370	0.375

Table 19: Point and interval estimates of σ, γ, $R(t)$, $h(t)$, and p from carbon fibers data

(p, v)	Par.	MLE		Bayes		ACI			BCI		
		Est.	SErr	Est.	SErr	Low.	Upp.	IL	Low.	Upp.	IL
S1	σ	3.4262	0.7906	3.4227	0.0981	1.8766	4.9757	3.0991	3.2319	3.6171	0.3852
	γ	6.0221	2.1827	6.0186	0.1005	1.7440	10.300	8.5560	5.8218	6.2162	0.3944
	$R(2)$	0.4289	0.1170	0.4298	0.0223	0.1996	0.6583	0.4587	0.3867	0.4742	0.0874
	$h(2)$	1.2778	0.4137	1.2759	0.0633	0.4670	2.0886	1.6215	1.1524	1.4019	0.2495
	p	0.2414	0.0795	0.2434	0.0963	0.0856	0.3971	0.3115	0.1094	0.4115	0.3021
S2	σ	4.5944	1.0221	4.5915	0.0987	2.5911	6.5977	4.0066	4.3990	4.7872	0.3882
	γ	6.2174	2.3000	6.2140	0.1006	1.7094	10.725	9.0160	6.0168	6.4118	0.3950
	$R(2)$	0.2269	0.1046	0.2276	0.0140	0.0220	0.4319	0.4099	0.2009	0.2557	0.0549
	$h(2)$	2.0142	0.5750	2.0124	0.0619	0.8872	3.1412	2.2540	1.8911	2.1348	0.2438
	p	0.7125	0.1250	0.7456	0.1884	0.5050	0.9950	0.4900	0.5478	0.9360	0.3881
S3	σ	5.0343	1.0904	5.0316	0.0988	2.8973	7.1714	4.2741	4.8392	5.2280	0.3887
	γ	7.6602	3.1681	7.6571	0.1007	1.4509	13.869	12.419	7.4595	7.8551	0.3956
	$R(2)$	0.2084	0.0987	0.2090	0.0129	0.0151	0.4018	0.3868	0.1844	0.2351	0.0507
	$h(2)$	2.2344	0.6116	2.2326	0.0625	1.0357	3.4331	2.3974	2.1100	2.3561	0.2460
	p	0.8629	0.0949	0.8921	0.0926	0.7141	0.9859	0.2719	0.7654	0.9959	0.2305
S4	σ	3.0615	0.6065	3.0580	0.0974	1.8727	4.2503	2.3776	2.8681	3.2509	0.3828
	γ	4.9874	1.6090	4.9837	0.1003	1.8338	8.1411	6.3073	4.7872	5.1807	0.3936
	$R(2)$	0.4498	0.0987	0.4506	0.0230	0.2564	0.6432	0.3868	0.4059	0.4963	0.0904
	$h(2)$	1.1188	0.3046	1.1170	0.0606	0.5217	1.7158	1.1941	0.9989	1.2381	0.2391
	p	0.2214	0.1265	0.2057	0.1529	0.0419	0.4479	0.4060	0.0318	0.4844	0.4526
S5	σ	4.2954	0.8335	4.2925	0.0983	2.6617	5.9291	3.2674	4.1013	4.4878	0.3865
	γ	5.8551	1.9926	5.8516	0.1005	1.9497	9.7604	7.8107	5.6548	6.0489	0.3942
	$R(2)$	0.2578	0.0912	0.2585	0.0155	0.0790	0.4366	0.3576	0.2288	0.2897	0.0609
	$h(2)$	1.8434	0.4598	1.8416	0.0620	0.9423	2.7445	1.8023	1.7201	1.9645	0.2444
	p	0.6757	0.1789	0.7873	0.2494	0.4494	0.9016	0.4522	0.5865	0.9906	0.4041
S6	σ	5.0290	0.9265	5.0263	0.0985	3.2131	6.8448	3.6317	4.8348	5.2217	0.3870
	γ	7.0941	2.5128	7.0909	0.1006	2.1690	12.019	9.8501	6.8937	7.2889	0.3952
	$R(2)$	0.1953	0.0806	0.1959	0.0122	0.0373	0.3533	0.3160	0.1726	0.2205	0.0479
	$h(2)$	2.2512	0.5171	2.2494	0.0614	1.2377	3.2647	2.0270	2.1289	2.3708	0.2419
	p	0.9215	0.1581	0.8976	0.4269	0.7901	0.9975	0.2074	0.8462	0.9955	0.1493

Based on Table 18, Fig. 6 confirms the existence and uniqueness of the fitted values $\hat{\sigma}$ and $\hat{\gamma}$, supporting the results reported in Table 19. To assess MCMC convergence, using S1 from Table 18, trace plots of σ, γ, $R(t)$, $h(t)$, and p over $\mathsf{H}^\bullet = 30,000$ Markov iterations are displayed in Fig. 7.

These plots demonstrate excellent convergence of the MCMC sampler and indicate that the posterior distributions of σ, γ, $h(t)$, and p are approximately symmetric, whereas $R(t)$ exhibits negative skewness.

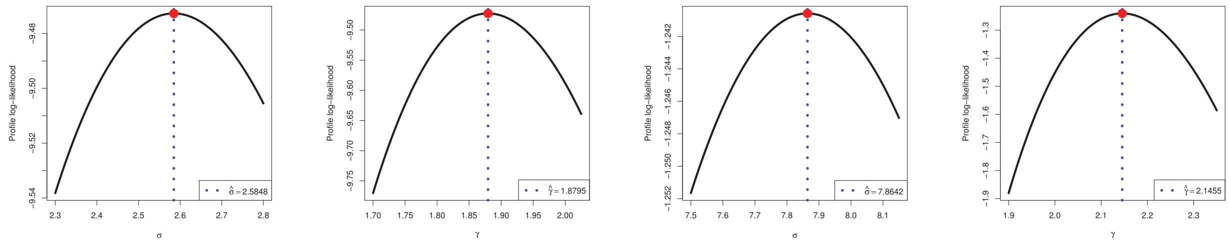

(a) S1 (b) S2

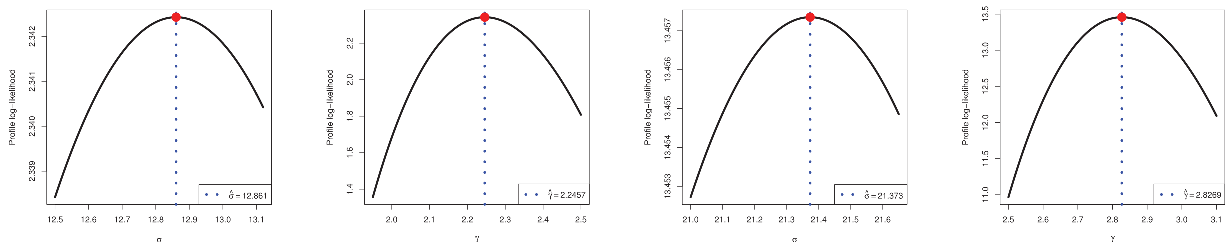

(c) S3 (d) S4

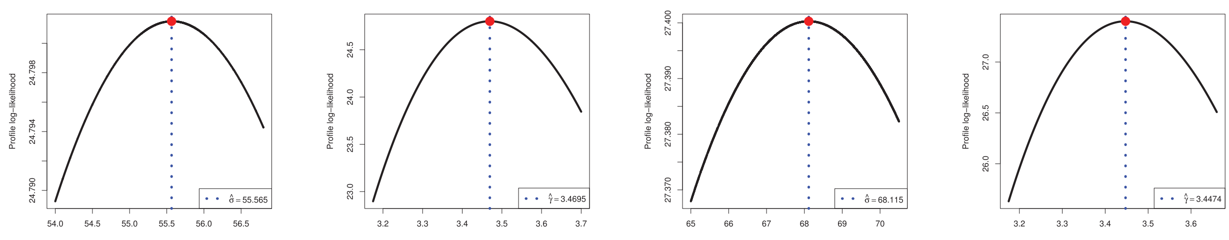

(e) S5 (f) S6

Figure 6: Profile log-likelihood curves of σ (left) and γ (right) from carbon fibers data (a–f)

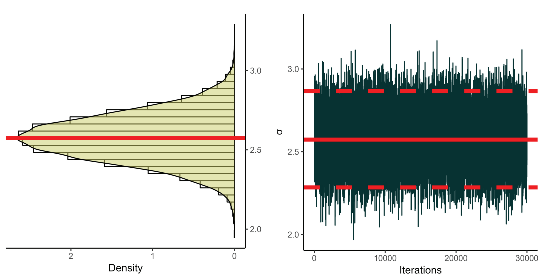

(a) σ

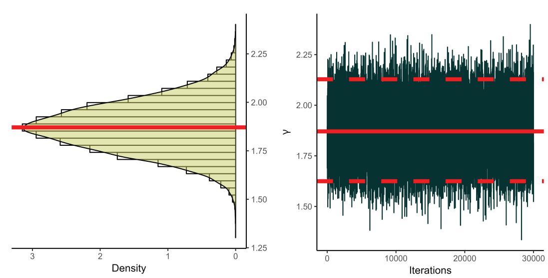

(b) γ

Figure 7: (Continued)

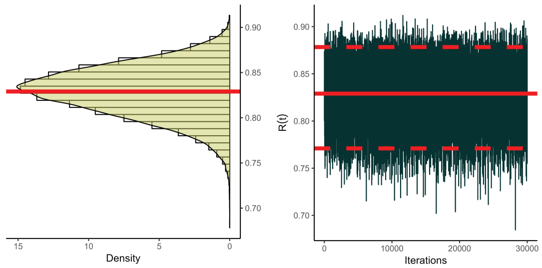

(c) $R(t)$

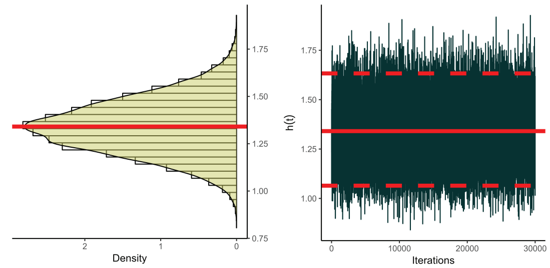

(d) $h(t)$

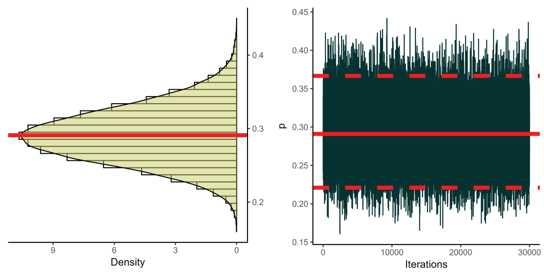

(e) p

Figure 7: The density and trace plots of (a): σ, (b): γ, (c): $R(t)$, (d): $h(t)$, and (e): p from carbon fibers

Consequently, the results from the carbon fibers dataset strongly validate the proposed estimation techniques. These findings are consistent with those obtained from the polyester fibers analysis, further highlighting the robustness and practical utility of the methods. Moreover, the outcomes demonstrate the adaptability of the proposed methodologies to different materials and experimental settings, underscoring their value in both research and applied contexts.

The proposed model supports (i) material design by enabling comparisons of fibers under uncertainty, (ii) maintenance planning through reliability and hazard function estimates that guide inspection or replacement policies, and (iii) reliability engineering by offering a cost-effective censoring framework applicable to broader systems beyond fibers.

7 Concluding Remarks

This study introduces a robust statistical framework for modeling lifetime data under an adaptive progressively hybrid censored scheme, leveraging the flexibility of the B12 distribution. By integrating both frequentist and Bayesian estimation approaches, the proposed methodology provides a comprehensive tool for accurate parameter estimation, particularly in complex real-world failure scenarios. The incorporation of MCMC techniques with informative priors further enhances estimation precision, demonstrating the practical effectiveness of the approach. Real-data applications to polyester and carbon fiber datasets highlight the model's adaptability: polyester fibers exhibit high durability and cost-efficiency, while carbon fibers offer exceptional strength, stiffness, and thermal resistance, making them relevant for advanced engineering applications. Across both datasets, the proposed model outperforms traditional approaches in capturing lifetime behaviors, offering valuable insights for reliability assessment, predictive maintenance, and risk management in engineering and biomedical contexts.

Acknowledgement: Not applicable.

Funding Statement: Princess Nourah bint Abdulrahman University Researchers Supporting Project number (PNURSP2025R50), Princess Nourah bint Abdulrahman University, Riyadh, Saudi Arabia.

Author Contributions: The authors confirm contribution to the paper as follows: study conception and design: Refah Alotaibi, Hoda Rezk, Ahmed Elshahhat; data collection: Refah Alotaibi; analysis and interpretation of results: Hoda Rezk, Ahmed Elshahhat; draft manuscript preparation: Refah Alotaibi, Hoda Rezk, Ahmed Elshahhat. All authors reviewed the results and approved the final version of the manuscript.

Availability of Data and Materials: The data that support the findings of this study are available within the paper.

Ethics Approval: Not applicable.

Conflicts of Interest: The authors declare no conflicts of interest to report regarding the present study.

References

1. Balakrishnan N, Cramer E. The art of progressive censoring. New York, NY, USA: Birkhäuser; 2014. doi:10.1007/978-0-8176-4807-7.
2. Kundu D, Joarder A. Analysis of Type-II progressively hybrid censored data. Comput Stat Data Anal. 2006;50(10):2509–28. doi:10.1016/j.csda.2005.05.002.
3. Childs A, Chandrasekar B, Balakrishnan N. Exact likelihood inference for an exponential parameter under progressive hybrid censoring schemes. In: Vonta F, Nikulin M, Limnios N, Huber-Carol C, editors. Statistical models and methods for biomedical and technical systems. Boston, MA, USA: Birkhäuser; 2008. p. 319–20. doi:10.1007/978-0-8176-4619-6_23.
4. Ng HKT, Kundu D, Chan PS. Statistical analysis of exponential lifetimes under an adaptive Type-II progressive censoring scheme. Nav Res Logistics. 2009;56(8):687–98. doi:10.1002/nav.20371.
5. Yuen HK, Tse SK. Parameter estimation for Weibull distributed lifetimes under progressive censoring with random removals. J Stat Comput Simul. 1996;55(1–2):57–71. doi:10.1080/00949659608811749.
6. Tse SK, Yang C, Yuen HK. Statistical analysis of Weibull distributed lifetime data under Type II progressive censoring with binomial removals. J Appl Stat. 2000;27(8):1033–43. doi:10.1080/02664760050173355.
7. Xiang L, Tse SK. Maximum likelihood estimation in survival studies under progressive interval censoring with random removals. J Biopharm Stat. 2005;15(6):981–91. doi:10.1080/10543400500266643.
8. Ding C, Yang C, Tse SK. Accelerated life test sampling plans for the Weibull distribution under Type I progressive interval censoring with random removals. J Stat Comput Simul. 2010;80(8):903–14. doi:10.1080/00949650902834478.
9. Afify WM. Statistical inference using progressively hybrid censored data under exponentiated exponential distribution with binomial random removals: theory and methods. S Afr Stat J. 2011;45(2):149–70.
10. Dey S, Kayal T, Tripathi YM. Statistical inference for the weighted exponential distribution under progressive Type-II censoring with binomial removal. Am J Math Manag Sci. 2018;37(2):188–208. doi:10.1080/01966324.2017.1395375.
11. Ashour SK, El-Sheikh AA, Elshahhat A. Inferences for Weibull parameters under progressively first-failure censored data with binomial random removals. Stat Optim Inf Comput. 2021;9(1):47–60. doi:10.19139/soic-2310-5070-611.

12. Walker PL, Thrower PA. Chemistry and physics of carbon. Boca Raton, FL, USA: CRC Press; 2021. doi:10.1201/9781003209065.
13. Deopura BL, Alagirusamy R, Joshi M, Gupta B. Polyesters and polyamides. Amsterdam, The Netherlands: Elsevier; 2008. doi:10.1201/9781439831861.
14. Burr IW. Cumulative frequency functions. Ann Math Stat. 1942;13(2):215–32. doi:10.1214/aoms/1177731607.
15. Goel R, Kumar K, Ng HKT, Kumar I. Statistical inference in Burr type XII lifetime model based on progressive randomly censored data. Qual Eng. 2024;36(1):150–65. doi:10.1080/08982112.2023.2276771.
16. Chakraborty T, Das S, Chattopadhyay S. A new method for generalizing burr and related distributions. Math Slovaca. 2022;72(1):241–64. doi:10.1515/ms-2022-0016.
17. Polosin VG, Mitroshin AN, Gerashchenko SI. Burr Type XII distribution in traffic control systems. Transp Res Proc. 2023;68:433–40. doi:10.1016/j.trpro.2023.02.058.
18. Elshahhat A, Nassar M. Analysis of adaptive Type-II progressively hybrid censoring with binomial removals. J Stat Comput Simul. 2023;93(7):1077–1103. doi:10.1080/00949655.2022.2127149.
19. Henningsen A, Toomet O. maxLik: a package for maximum likelihood estimation in R. Comput Stat. 2011;26(3):443–58. doi:10.32614/cran.package.maxlik.
20. Greene WH. Econometric analysis. 4th. Hoboken, NJ, USA: Prentice-Hall; 2000. doi:10.1007/s00362-010-0315-8.
21. Plummer M, Best N, Cowles K, Vines K. CODA: convergence diagnosis and output analysis for MCMC. R News. 2006;6(1):7–11. doi:10.32614/cran.package.coda.
22. Kundu D. Bayesian inference and life testing plan for the Weibull distribution in presence of progressive censoring. Technometrics. 2008;50(2):144–54. doi:10.1198/004017008000000217.
23. Irfan M, Dutta S, Sharma AK. Statistical inference and optimal plans for improved adaptive Type-II progressive censored data following Kumaraswamy-G family of distributions. Phys Scr. 2025;100(2):025213. doi:10.1088/1402-4896/ada216.
24. Kavianihamedani H, Quinn JD, Smith JD. New diagnostic assessment of MCMC algorithm effectiveness, efficiency, reliability, and controllability. IEEE Access. 2024;12(1):42385–42400. doi:10.1109/ACCESS.2024.3378752.
25. Nichols MD, Padgett WJ. A bootstrap control chart for Weibull percentiles. Qual Reliab Eng Int. 2006;22(2):141–51. doi:10.1002/qre.691.